

Distributed Event-triggered Fault-tolerant Consensus Control of Multi-agent Systems under DoS Attacks

Chun Liu, Bin Jiang, *Fellow, IEEE*, Yang Li, and Ron J. Patton, *Life Fellow, IEEE*

Abstract—This study investigates the distributed fault-tolerant consensus issue of multi-agent systems subject to complicated abrupt and incipient time-varying actuator faults in physical hierarchy and aperiodic denial-of-service (DoS) attacks in networked hierarchy. Decentralized estimators are devised to estimate consecutive system states and actuator faults. A unified framework with an absolute local output-based closed-loop estimator in decentralized fault estimation design and a relative broadcasting state-based open-loop estimator in distributed event-triggered fault-tolerant consensus design is developed. Criteria of exponential consensus of the faulty multi-agent systems under DoS attacks are derived by virtue of average dwelling time and attack frequency technique. Simulations are outlined to confirm the efficacy of the proposed distributed fault-tolerant consensus control algorithm based on an event-triggered mechanism.

Index Terms—Distributed fault-tolerant consensus control, event-triggered mechanism, multi-agent systems, incipient and abrupt actuator faults, DoS attacks.

I. INTRODUCTION

DISTRIBUTED consensus control of networked multi-agent system (MASs) has witnessed a substantial surge in interest and made swift progress in the field of civil-military integration because of its distributed advantages of comprehensive cooperation and autonomy. A concise examination of the coordination and consensus of MASs was outlined in [1]. Recently, there has been a notable curiosity in achieving distributed consensus for the linear/nonlinear MASs [2], [3] and homogeneous/heterogeneous MASs [4], [5]. The achievement of consensus in MASs requires precise and ongoing interaction among individuals through communication topologies. Any compromise to this essential information exchange, particularly due to cyber-attacks, can disrupt the consensus achieved [6]. Thus, the network security management of MASs becomes highly coveted in light of diverse cyber-attacks, such as false data-injection attacks [7], [8], deception attacks [9] and DoS attacks [10], [11]. Different from destroying the integrity of input and output signal (deception attacks), periodic/aperiodic DoS attacks [10], [12] and strategic DoS attacks [13] in MASs

lead to interruption of information transmission between sensor and control channels. However, for directed/undirected balanced graph or fixed/switching topology [14], the existing graph theory and switching concept can not directly solve the consensus control problem affected by intermittent network interruption of MASs under DoS attacks. Therefore, developing a novel distributed anti-attack consensus control for MASs against DoS attacks is necessary but also presents a challenge.

The dynamic evolution of MASs is influenced not only by adversarial DoS attacks in networked hierarchy but also by actuator faults at the local agent level in physical hierarchy. Therefore, it is desirable that MASs operate safely and reliably, and fault-tolerant consensus control (FTCC) [15]-[17] is a powerful method to attain local adaptability and global coordination expected by MASs with appropriate anti-attack effectiveness. Aiming at heterogeneous nonlinear MASs, a robust adaptive FTCC protocol was developed to realize fault-tolerant consensus by local (adjacent) state information and compensate for complex uncertainties and unpredictable actuator faults [18]. The limited output information-based distributed fault-tolerant tracking scheme was put forward for uncertain MASs based upon neural network adaptive learning algorithm [19]. However, most studies focus on abrupt actuator faults that are constant, time-varying or dead-zone constraints [18], [20], while ignoring incipient actuator faults in beginning stage. It is noteworthy that the large-scale collapse of MASs may be caused by a single agent spreading incipient early faults to its neighbors through topological networks even under DoS attacks. It is exceedingly arduous to achieve the desired consensus of MASs against diverse abrupt and incipient actuator faults through the existing FTCC techniques.

Overall, fault-tolerant consensus issue of MASs under deception attacks [21], [22] or false data injection attacks [23] has been partially investigated, which is similar to modeling the loss of data integrity in networked hierarchy as the simple superposition or deletion of faults in physical hierarchy. However, due to the difficulty of direct transmission interruption under DoS attacks, few studies pay attention to an FTCC protocol, particularly in scenarios involving concurrent abrupt and incipient faults and DoS attacks. At present, there are limited literature about FTCC method of synchronously compensating actuator faults and resisting DoS attacks in MASs, with the following emphasis. The distributed observer-based tolerant control was designed for linear MASs with actuator faults to ensure the exponential stability even under DoS attacks [24]. For the heterogeneous MASs [25], integral quadratic constrained nonlinear MASs [26], and switched nonlinear uncertain MASs [27], Lyapunov stability and average dwelling

This work was supported by National Natural Science Foundation of China (62103250, 62333011, and 62336005); Shanghai Sailing Program (21YF1414000); Project of Science and Technology Commission of Shanghai Municipality, China (22JC1401401). (*Corresponding author: Bin Jiang.*)

C. Liu and Y. Li are with the School of Mechatronic Engineering and Automation, Shanghai University, Shanghai 200444, China (e-mail: Chun_Liu@shu.edu.cn, yongerli@shu.edu.cn).

B. Jiang is with the College of Automation Engineering, Nanjing University of Aeronautics and Astronautics, Nanjing 210016, China (e-mail: binjiang@nuaa.edu.cn).

R. J. Patton is with the School of Engineering, University of Hull, Hull HU6 7RX, U.K. (e-mail: r.j.patton@hull.ac.uk).

time (ADT) technique were utilized to resist both DoS attacks and actuator faults via FTCC technique. On the one hand, most distributed FTCC studies are either based on output-feedback control [5], [10] or neighborhood state information [14], [18]. The FTCC schemes without absolute state/output information under DoS attacks are rarely explored, and a novel estimator capable of storing successfully transmitted broadcasting information within DoS attacks sleeping duration is urgently needed. On the other hand, an in-depth analysis of event-triggered consensus of MASs subject to DoS attacks is performed [28], [29], since it can synchronize all individuals effectively, even in cases where message transmission fails intermittently, by reducing computational resources and communication load substantially [30]-[32]. The distributed cooperative event-triggered consensus control schemes were proposed for MASs when encountering cyclic DoS jamming attacks [33], aperiodic time-sequence-based DoS attacks [34] or unpredicted faults [35]. Hence, it is crucial to devise a local output and broadcasting state estimation-driven FTCC algorithm coupled with an event-triggered mechanism for MASs confronting complex time-varying actuator faults to address the anti-attack resilience problem amidst aperiodic DoS attacks.

The primary innovations are emphasized as follows. (i) Compared with the consensus of MASs under independent attacks [12], [28] or the FTCC strategies compensating traditional bias faults or loss of effectiveness [25], [26], this study attempts to effectively implement dual security guarantees in cyber-physical MASs: fault tolerance and attack resilience. It is a comprehensive endeavor to address the composite self-constraints (abrupt and incipient faults) in the physical layer and the paralyzed connectivities (DoS attacks) in the networked layer through the local/broadcasting estimation-based distributed event-triggered FTCC mechanism. (ii) Different from considering periodic energy-limited DoS attacks [12], [33], the aperiodic DoS attacks with specific attack frequency, attack duration, and ADT can be effectively defended against. A novel control structure is developed, combining the benefits of an absolute local output-based closed-loop estimator (ALO-CLE) in the decentralized fault estimation (FE) and a relative broadcasting state-based open-loop estimator (RBS-OLE) in the distributed event-triggered FTCC. The interrupt state information of the triggering function in the current DoS attack interval is replaced by the distributed adjacency broadcasting information from an open-loop estimator.

The remainder of this study is structured. Problem formulation with MASs description, actuator fault modeling, and DoS attacks modeling is provided in Section II. ALO-CLE-based decentralized FE and RBS-OLE-based distributed event-triggered FTCC designs are proposed to attain the exponential consensus of MASs in Sections III. The simulation is demonstrated in Section IV to validate the efficacy of the proposed FTCC algorithm. Ultimately, the conclusions are summarized in Section V.

Notations: \mathbb{R}, \mathbb{N} refer to the sets of real and natural numbers, respectively. The symbol \otimes denotes the Kronecker product. $\lambda_{\max}(\cdot), \lambda_{\min}(\cdot)$ represent the maximum and minimum eigenvalues, and $x = \text{col}(x_i) = [x_1^T, \dots, x_N^T]^T, i = 1, \dots, N$.

II. PRELIMINARIES AND PROBLEM FORMULATION

A. MASs with actuator fault modeling

Consider the following dynamics of the i th agent in the faulty MASs ($i = 1, \dots, N$),

$$\begin{aligned} \dot{x}_i(t) &= Ax_i(t) + Bu_i(t) + Ff_i(t) + D_1d_{i1}(t) \\ y_i(t) &= Cx_i(t) + D_2d_{i2}(t) \end{aligned} \quad (1)$$

where $x_i(t) \in \mathbb{R}^n, y_i(t) \in \mathbb{R}^p, u_i(t) \in \mathbb{R}^m$ and $f_i(t) \in \mathbb{R}^q$ are the system state, output, input and actuator fault, respectively, $d_{i1}(t) \in \mathbb{R}^{s_1}$ and $d_{i2}(t) \in \mathbb{R}^{s_2}$ denote the disturbances in the input and output channels, A, B, C, F, D_1 and D_2 are given system/fault/disturbance matrices, $f_i(t) = [f_{i1}^T, \dots, f_{iq}^T]^T$ denotes the complicated abrupt and incipient actuator fault, and each element $f_{is}(t), s = 1, \dots, q$ can be represented by

$$f_{is}(t) = (1 - e^{-\epsilon_s(t-T_s)})\bar{f}_{is}, t \geq T_s, s = 1, \dots, q \quad (2)$$

where T_s denotes the complicated fault occurrence moment, \bar{f}_{is} denotes the s th constant fault bound, and ϵ_s denotes the unknown decay rate. The actuator fault is classified as an incipient fault when $\underline{\epsilon}_{\text{inc}} \leq \epsilon_s < \bar{\epsilon}_{\text{inc}}$ (with a *slow decay rate*) and an abrupt fault when $\epsilon_s \geq \bar{\epsilon}_{\text{inc}}$ (with a *quick decay rate*), respectively.

Assumption 2.1: The dynamics (A, B) and (A, C) are controllable and observable, respectively.

Assumption 2.2: (i) The abrupt and incipient fault exhibits distinguishable characteristics following each fault occurrence event. (ii) The upper and lower limits of the incipient fault are manually determined using the given positive constants $\bar{\epsilon}_{\text{inc}}$ and $\underline{\epsilon}_{\text{inc}}$, respectively.

Assumption 2.3: The disturbance $d_{i2}(t)$ in the output channel is constrained within the known and positive upper bound, i.e., $\|\dot{d}_{i2}(t)\| \leq \bar{d}_{i2}, i = 1, \dots, N$.

Remark 2.1: (i) Assumption 2.1 provides the controllable and observable conditions of MASs and guarantees the abrupt and incipient actuator faults $f_i(t)$ to be constrained in a given tolerance range with the designed control law $u_i(t)$. (ii) In particular for abrupt time-varying actuator faults, when the decay rate ϵ_s is large enough, the mutation is completed at the respective pulse moment and the abrupt fault is essentially a class of actuator stuck faults, i.e., $f_{is}(t) = (1 - e^{-\epsilon_s(t-T_s)})\bar{f}_{is} \cong \bar{f}_{is}$. Moreover, the abrupt fault can be equated to a typical partial loss of effectiveness $f_{is}(t) = (1 - e^{-\epsilon_s(t-T_s)})k_i\bar{f}_{is} \cong k_i\bar{f}_{is}$ with the large enough ϵ_s . Hence, the abrupt and incipient time-varying actuator faults can be equated to typical stuck and partial loss of effectiveness faults, but not to saturation faults, which is the crucial discrepancy from typical actuator faults.

B. DoS attacks modeling

Generally speaking, malicious attackers with limited resources usually choose to launch intermittent DoS attacks on the communication network of MASs during the time-varying activation period of attacks, and at the same time, they will terminate DoS attacks at intervals and keep sleeping/dormant, so as to accumulate energy for the next DoS attacks. For given $t \geq t_0 \in \mathbb{R}$, suppose that there exists a $r \in \mathbb{N}$, positive spans Δ_r and Δ_r^a , and signify $\{t_r^a\}_{r \in \mathbb{N}}$ as an aperiodic sampled-data DoS attack sequence over $[t_0, t)$ when the DoS attacker

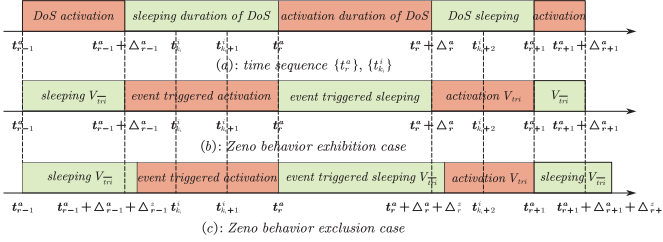


Fig. 1. Time intervals of DoS activation, DoS sleeping, event-triggered activation and event-triggered sleeping.

activates at t_r^a and $t_{r+1}^a = t_r^a + \Delta_r$ with the time-varying aperiodic sampling interval Δ_r . The r th DoS time interval is denoted as $\Gamma_r^a = [t_r^a, t_{r+1}^a)$ with $t_{r+1}^a > t_r^a + \Delta_r^a$. Suppose that there is an infinite sequence of non-overlapping time intervals, uniformly bounded as $[t_r^a, t_r^a + \Delta_r^a)$ and $[t_{r-1}^a + \Delta_{r-1}^a, t_r^a)$, during which the graph remains unchanged in terms of time.

Definition 2.1: Denote $\Gamma^a(t_0, t) = \cup \Gamma_r^a \cap [t_0, t]$, $r \in \mathbb{N}$ as the total activation duration of DoS attacks over $[t_0, t)$, and denote $\Gamma^s(t_0, t) = [t_0, t] \setminus \Gamma^a(t_0, t)$ as the total sleeping duration of DoS attacks over $[t_0, t)$ in which information transmission is allowed. For $\Gamma^s(t_0, t)$, assume that there exists a natural number k_i such that $\{t_{k_i}^i\}_{k_i \in \mathbb{N}}$ represents an event-triggered sampled-data control sequence over the interval $[t_0, t)$, where the i -th updated controller activates at time $t_{k_i}^i$. Furthermore, denote $N_\Gamma(t_0, t) = N_{\Gamma^a}(t_0, t) + N_{\Gamma^s}(t_0, t)$, $\forall t > t_0 \geq 0$, where $N_{\Gamma^a}(t_0, t)$ and $N_{\Gamma^s}(t_0, t)$ are the numbers of DoS activation and sleeping attacks.

Definition 2.2 (DoS attack frequency): denote $\mathcal{F}_{\Gamma^a}(t_0, t) = \frac{N_{\Gamma^a}(t_0, t)}{t - t_0}$ as the DoS attack frequency over $[t_0, t)$ for all $t \geq t_0$.

Definition 2.3 (DoS attack duration): for $\Gamma^a(t_0, t) = \cup \Gamma_r^a \cap [t_0, t]$, $r \in \mathbb{N}$, there exists a chattering bound $\Gamma_0 \geq 0$ and ADT $\tau_a > 0$ such that $\Gamma^a(t_0, t) = \sum_{r \in \mathbb{N}} \Delta_r^a \leq \Gamma_0 + \frac{t - t_0}{\tau_a}$.

Control objective: The exponential average consensus control issue of the faulty MASs in (1) is addressed when, for all $t \geq t_0$, there exists a positive amplitude μ and a positive decay rate λ such that $\|x_i(t) - \frac{1}{N} \sum_{i=1}^N x_i(t)\|^2 \leq \mu e^{-\lambda(t-t_0)} \|x_i(t_0) - \frac{1}{N} \sum_{i=1}^N x_i(t_0)\|^2$.

Remark 2.2: The time sequences $\{t_r^a\}_{r \in \mathbb{N}}$ and $\{t_{k_i}^i\}_{k_i \in \mathbb{N}}$ are depicted in Fig. 1(a), in which the event-triggered mechanism holds sleeping during DoS attack activation interval and is activated in DoS attack sleeping duration. For the case of Zeno behavior exhibition and exclusion in Fig. 1(b), (c), two types of Lyapunov functions V_{tri} and $V_{tr\bar{i}}$ are selected, and the specific analysis with each upper bound of interexecution interval Δ_r^z , $r \in \mathbb{N}$ is discussed in the following section.

Remark 2.3: Communication topologies in MASs may be frequently subjected to DoS attacks (link-break failures) and malicious attacker tries to block the agent-to-agent information transmission, thus leading to connection paralysis and poor consensus in the coordination process [6]. In the case of DoS attacks [12], [33], the interaction of control data is suspended as the control channel is compromised by smart opponents, so it is necessary to assume that the considered attacks can be recoverable and to redefine the scheduling of the controller updating time instants. In contrast to periodic DoS attacks observed in well-known deterministic attack strategies [34],

the DoS attacks orchestrated by the adversary are simulated to occur in an aperiodic manner and tend to disrupt the control channel. However, it is assumed that certain smart devices can effortlessly identify the uniform bounds of DoS attack duration and frequency.

III. MAIN RESULTS

This section provides an integrated co-design of FE and FTCC strategy to deal with MASs against complicated abrupt and incipient actuator faults under DoS attacks in consensus control field. By incorporating estimation error, event-triggered error, and average state consensus error into the carefully selected Lyapunov function, the challenge of consensus control is addressed using a distributed event-triggered FTCC scheme based on RBS-OLE, leveraging local state and fault estimations from ALO-CLE in FE design and neighboring broadcast information during event-triggered occurrences. The control structure, which encompasses ALO-CLE-based decentralized FE design and RBS-OLE-based distributed FTCC design, addresses issues arising from actuator faults and aperiodic DoS attacks within physical and networked hierarchies, as depicted in Fig. 2.

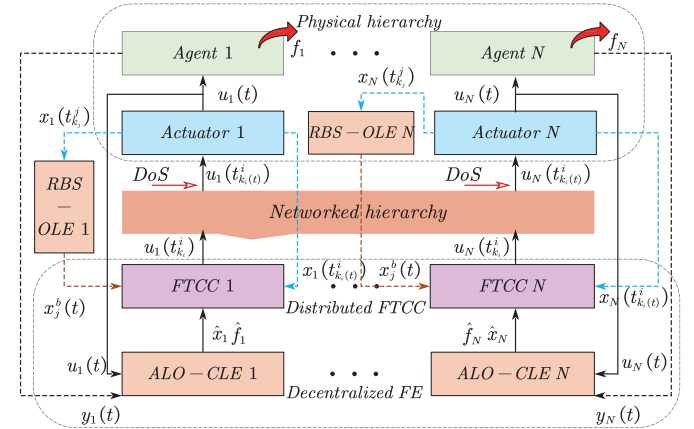


Fig. 2. The structure with ALO-CLE-based decentralized FE and RBS-OLE-based distributed FTCC in physical and networked hierarchies.

A decentralized ALO-CLE-based FE is first proposed for MASs to receive the estimated state and fault information in a pure-feedback fashion in the following FTCC design. Define the augmented state as $\bar{x}_i(t) = [x_i^T(t) \ f_i^T(t) \ d_{i2}^T(t)]^T$ and the induced disturbance as $\bar{d}_i(t) = [d_{i1}^T(t) \ \hat{f}_i^T(t) \ d_{i2}^T(t)]^T$. The i th augmented systems are reformulated as

$$\dot{\bar{x}}_i(t) = \bar{A} \bar{x}_i(t) + \bar{B} u_i(t) + \bar{D} \bar{d}_i(t), \quad y_i(t) = \bar{C} \bar{x}_i(t) \quad (3)$$

where $\bar{A} = [A \ F \ \mathbf{0}_{n \times s_2}; \ \mathbf{0}_q \times n \ \mathbf{0}_q \ \mathbf{0}_q \times s_2; \ \mathbf{0}_{s_2 \times n} \ \mathbf{0}_{s_2 \times q} \ \mathbf{0}_{s_2}]$, $\bar{B} = [B; \ \mathbf{0}_q \times m; \ \mathbf{0}_{s_2 \times m}]$, $\bar{D} = [D_1 \ \mathbf{0}_{n \times q} \ \mathbf{0}_{n \times s_2}; \ \mathbf{0}_q \times s_1 \ I_q \ \mathbf{0}_q \times s_2; \ \mathbf{0}_{s_2 \times s_1} \ \mathbf{0}_{s_2 \times q} \ I_{s_2}]$, and $\bar{C} = [C \ \mathbf{0}_{p \times q} \ D_2]$.

Each augmented state $\bar{x}_i(t)$ can be estimated by the corresponding decentralized ALO-CLE:

$$\begin{cases} \dot{z}_i(t) = L z_i(t) + G u_i(t) + J y_i(t) \\ \hat{\bar{x}}_i(t) = z_i(t) + H y_i(t) \end{cases} \quad (4)$$

where $z_i(t) \in \mathbb{R}^{n+q+s_2}$ is the state of ALO-CLE, $\hat{\bar{x}}_i(t) = [\hat{x}_i^T(t) \ \hat{f}_i^T(t) \ \hat{d}_{i2}^T(t)]^T$ is the augmented state estimation with

the state estimation $\hat{x}_i(t) \in \mathbb{R}^n$, the fault estimation $\hat{f}_i(t) \in \mathbb{R}^q$, and the output disturbance estimation $\hat{d}_{i2}(t) \in \mathbb{R}^{s_2}$, and L, G, J, H are adequate matrices to be designed.

Denote the estimation error as $\bar{e}_i(t) = \bar{x}_i(t) - \hat{x}_i(t) = [e_{x_i}^T(t) \ e_{f_i}^T(t) \ e_{d_{i2}}^T(t)]^T$ with $e_{x_i}(t) = x_i(t) - \hat{x}_i(t)$, $e_{f_i}(t) = f_i(t) - \hat{f}_i(t)$, and $e_{d_{i2}}(t) = d_{i2}(t) - \hat{d}_{i2}(t)$.

Define $M = I_{n+q+s_2} - HC$ and $J = J_1 + J_2$, and the estimation error systems are obtained as

$$\begin{aligned} \dot{\bar{e}}_i(t) &= (M\bar{A} - J_1\bar{C})\bar{e}_i(t) + (M\bar{B} - G)u_i(t) \\ &\quad + (M\bar{A} - J_1\bar{C} - L)z_i(t) + M\bar{D}\bar{d}_i(t) \\ &\quad + ((M\bar{A} - J_1\bar{C})H - J_2)y_i(t) \end{aligned} \quad (5)$$

Then, with the equality constraints of matrices L, G, J_1, J_2 and H as follows,

$$L = M\bar{A} - J_1\bar{C}, J_2 = LH, G = M\bar{B} \quad (6)$$

where L is Hurwitz, and it hence follows that $\dot{\bar{e}}_i(t) = L\bar{e}_i(t) + M\bar{D}\bar{d}_i(t)$ with the following global dynamics:

$$\dot{\bar{e}}(t) = (I_N \otimes L)\bar{e}(t) + (I_N \otimes M\bar{D})\bar{d}(t) \quad (7)$$

where $\bar{e}(t) = \text{col}(\bar{e}_i(t))$ and $\bar{d}(t) = \text{col}(\bar{d}_i(t))$, $i = 1, \dots, N$.

To address the issue of wasted or unnecessary utilization of communication resources, an event-triggered control operation is employed to update the control signal, utilizing a threshold mechanism linked to adjacency broadcasting information. Since $\{t_0^i, t_1^i, \dots, t_{k_i}^i, \dots\}$ is denoted as the event-triggered control sequence over $[t_0, t)$ for $\Gamma^s(t_0, t)$ when the i th agent can actively update. For $t \in [t_{k_i}^i, t_{k_i+1}^i)$, the fault-tolerant consensus controller in the distributed manner is devised as

$$u_i(t) = -K_1\hat{x}_i(t) + K_2\Xi_i(x_{j \in \mathcal{N}_i}^b(t)) \quad (8)$$

where $K_1 = [K_x \ K_f \ \mathbf{0}_{m \times s_2}]$ is the compensation-based estimating matrix with the state-estimation matrix $K_x \in \mathbb{R}^{m \times n}$ and the fault-estimation matrix $K_f \in \mathbb{R}^{m \times q}$, and $K_2 \in \mathbb{R}^{m \times n}$ is the adjacency information-based broadcasting matrix. The distributed adjacency broadcasting value $\Xi_i(x_{j \in \mathcal{N}_i}^b(t))$ in (8) is designed as follows:

$$\Xi_i(x_{j \in \mathcal{N}_i}^b(t)) = \sum_{j \in \mathcal{N}_i} a_{ij} (x_j^b(t) - x_i^b(t)) \quad (9)$$

where a_{ij} is the (i, j) th entry of \mathcal{A} with graph \mathcal{G} , and $x_i^b(t) = x_i(t_{k_i}^i)$ is denoted as the latest triggering state of the i th agent with the subscript $k_i(t)$ described as the last successful triggering time instant as follows:

$$k_i(t) = \begin{cases} -1, & \text{when } \Gamma^s(t_0, t) = \emptyset \\ \sup\{k_i \in \mathbb{N} \mid t_{k_i}^i \in \Gamma^s(t_0, t)\}, & \text{otherwise} \end{cases} \quad (10)$$

which implies that the distributed adjacency broadcasting information is not required with $\Xi_i(x_{j \in \mathcal{N}_i}^b(t_{k_i}^i)) = -\sum_{j \in \mathcal{N}_i} a_{ij} x_i^b(t_{k_i}^i)$ when there are no DoS sleeping attacks.

For the neighboring agent, $x_j^b(t)$ is denoted as the adjacency broadcasting state of the designed RBS-OLE of the j th agent, and for $t \in [t_{k_j}^j, t_{k_j+1}^j)$, the adjacency broadcasting state dynamics of RBS-OLE are formulated as

$$\dot{x}_j^b(t) = Ax_j^b(t), x_j^b(t_{k_j}^j) = x_j(t_{k_j}^j) \quad (11)$$

Define the event-triggered error as $\delta_i(t) = x_i^b(t) - x_i(t)$. In order to specify the event-triggered time sequence $\{t_{k_i}^i\}_{k_i \in \mathbb{N}}$,

the event-triggered mechanism imposes the constraint $\delta_i(t)$, such that $\|\delta_i(t)\| \leq \theta_i \|\Xi_i(x_{j \in \mathcal{N}_i}^b(t))\|$, where $\theta_i > 0$ is the threshold. This ensures that the updated FTCC law $u_i(t)$ in (8) can be triggered successfully during the dormant phase of DoS attacks only if the event-triggered error $\delta_i(t)$ falls below the threshold function of the adjacency broadcasting message.

Remark 3.1: The augmented state estimator $-K_1\hat{x}_i(t)$ is time-triggered and provides valuable data for control inputs sustainably. However, the adjacency broadcasting value $K_2\Xi_i(x_{j \in \mathcal{N}_i}^b)$ among agents is event-triggered, and its loss is related to both DoS attacks and event-triggered instance. In the presence of DoS attacks, the adjacency broadcasting value cannot effectively transmit, and the event-triggered mechanism fails to operate. In the absence of DoS attacks, the adjacency data is determined by the event-triggered mechanism. Under this strategy, event triggers and DoS attacks cannot occur simultaneously, and there is no need to distinguish whether packet loss is caused by DoS attackers or event triggers. Furthermore, to trace the missing data packet, an existing DoS attack detection mechanism [29] can be utilized.

The i th faulty dynamics in (1) are rewritten as

$$\begin{aligned} \dot{x}_i(t) &= (A - BK_x)x_i(t) + BK_1\bar{e}_i(t) + D_1d_{i1}(t) \\ &\quad + BK_2 \sum_{j \in \mathcal{N}_i} a_{ij} (x_j(t) - x_i(t)) \\ &\quad + BK_2 \sum_{j \in \mathcal{N}_i} a_{ij} (\delta_j(t) - \delta_i(t)) \end{aligned} \quad (12)$$

It then follows that

$$\begin{aligned} \dot{x}(t) &= [I_N \otimes (A - BK_x) - \mathcal{L} \otimes BK_2]x(t) \\ &\quad + (I_N \otimes D_1)d_1(t) + (I_N \otimes BK_1)\bar{e}(t) - (\mathcal{L} \otimes BK_2)\delta(t) \end{aligned} \quad (13)$$

where $x(t) = \text{col}(x_i(t))$, $d_1(t) = \text{col}(d_{i1}(t))$, $\delta(t) = \text{col}(\delta_i(t))$, and \mathcal{L} is represented as the Laplacian matrix.

Denote the average state consensus error as $e_i(t) = x_i(t) - \frac{1}{N} \sum_{i=1}^N x_i(t)$ and the global vector as $e(t) = \text{col}(e_i(t))$, and it is then obtained as $e(t) = (\Theta \otimes I_n)x(t)$ with $\Theta = I_N - \frac{1}{N} \mathbf{1}_N \mathbf{1}_N^T$.

Theorem 3.1: For the undirected and connected graph \mathcal{G} , there exists an orthogonal matrix $\Psi = [\frac{1}{\sqrt{N}} \psi_2 \ \psi_3 \ \dots \ \psi_N] \in \mathbb{R}^{N \times N}$ such that $\Psi\Psi^T = I_N$ and $\mathcal{L}\Theta = \Theta\mathcal{L} = \mathcal{L}$, where $\psi_i \in \mathbb{R}^N$, $i = 2, \dots, N$ is an orthogonal eigenvector of Laplacian matrix \mathcal{L} corresponding with $\lambda_i(\mathcal{L})$, i.e., $\mathcal{L}\psi_i = \lambda_i(\mathcal{L})\psi_i$. Furthermore, denote $\psi = [\psi_2 \ \psi_3 \ \dots \ \psi_N] \in \mathbb{R}^{N \times (N-1)}$, and it is derived as $\psi\psi^T = \Theta$.

Proof: By the definition of the orthogonal matrix $\Psi = [\frac{1}{\sqrt{N}} \psi_2 \ \psi_3 \ \dots \ \psi_N]$, it is easy to obtain that $\Psi\Psi^T = \frac{1}{N} \mathbf{1}_N \mathbf{1}_N^T + \psi_2\psi_2^T + \dots + \psi_N\psi_N^T = I_N$. Then, $\psi\psi^T = I_N - \frac{1}{N} \mathbf{1}_N \mathbf{1}_N^T = \Theta$ is proved. With the definition of $\mathcal{L}\psi_i = \lambda_i(\mathcal{L})\psi_i$, it follows that

$$\begin{aligned} \mathcal{L}\Theta &= \mathcal{L}\psi_2\psi_2^T + \dots + \mathcal{L}\psi_N\psi_N^T \\ &= \lambda_2(\mathcal{L})\psi_2\psi_2^T + \dots + \lambda_N(\mathcal{L})\psi_N\psi_N^T = \mathcal{L} \\ &= \psi_2\psi_2^T \mathcal{L} + \dots + \psi_N\psi_N^T \mathcal{L} = \Theta\mathcal{L} \end{aligned} \quad (14)$$

It thus follows that

$$\begin{aligned} \dot{e}(t) &= [I_N \otimes (A - BK_x) - \mathcal{L} \otimes BK_2]e(t) \\ &\quad + (\Theta \otimes D_1)d_1(t) + (\Theta \otimes BK_1)\bar{e}(t) - (\mathcal{L} \otimes BK_2)\delta(t) \end{aligned} \quad (15)$$

The objective of the distributed event-triggered FTCC design (8), (9) aims at determining H, J_1, K_x, K_f and K_2 such that the exponential consensus problem of the MASs (1) subject to the aperiodic DoS attacks in networked layer and the

complicated incipient and abrupt actuator faults (2) in physical layer is effectively solved.

Theorem 3.2: Given positive constants $\gamma_1, \gamma_2, \epsilon_{\text{inc}}, \eta_\Gamma$ and a positive chattering bound Γ_0 , the MASs with the distributed FTCC protocol (8)-(11) under the event-triggered mechanism $\|\delta_i(t)\| \leq \theta_i \|\Xi_i(x_{j \in \mathcal{N}_i}^b(t))\|$ can obtain the exponential consensus efficiency, if there exist symmetric positive-definite matrices $P_1, P_2 \in \mathbb{R}^{n \times n}$, positive matrices $Q_1, Q_2, Q_3 \in \mathbb{R}^{n \times n}$, $R \in \mathbb{R}^{m \times m}$, matrices $K_x \in \mathbb{R}^{m \times n}$, $H \in \mathbb{R}^{(n+q+s_2) \times p}$, $J_1 \in \mathbb{R}^{(n+q+s_2) \times p}$ such that

$$-Q_1 - P_1 B K_x - K_x^T B^T P_1 + Q_2 < 0 \quad (16)$$

$$L + L^T + M \bar{D} \bar{D}^T M^T + \min\{\eta_{\alpha_1}, \eta_{\alpha_2}\} I_{n+q+s_2} < 0 \quad (17)$$

$$P_2 A + A^T P_2 - P_2 B K_x - K_x^T B^T P_2 + Q_3 < 0 \quad (18)$$

where $\eta_{\alpha_1} = \frac{\gamma_1 k_1 \omega_1^2 \lambda_{\max}^2(\Theta)}{\lambda_{\min}(Q_2)} + \alpha_1$ and $\eta_{\alpha_2} = \frac{\gamma_1 k_3 \omega_3^2 \lambda_{\max}^2(\Theta)}{\lambda_{\min}(Q_3)} - \alpha_2$ with the positive scalars α_1 and α_2 satisfied with $\alpha_1 \leq \frac{(k_1 k_2 k'_1 - k_2 k'_1 - k_1 k'_1 - k_1 k_2) \lambda_{\min}(Q_2)}{k_1 k_2 k'_1 \lambda_{\max}(P_1)} - \frac{2k_2 \omega_2^2 \lambda_N^4(\mathcal{L}) \bar{\theta}^2}{(1-2\theta^2 \lambda_N^2(\mathcal{L})) \lambda_{\min}(Q_2) \lambda_{\max}(P_1)}$, $\alpha_2 \geq \frac{(k_3 k'_2 - k_2 - k_3) \lambda_{\min}(Q_3)}{k_3 k'_2 \lambda_{\min}(P_2)}$ and $\min\{2\epsilon_{\text{inc}} - \alpha_1, 2\epsilon_{\text{inc}} + \alpha_2\} \geq \frac{\gamma_2}{\gamma_1}$. Furthermore, the positive scalars k_1, k_2, k_3, k'_1 and k'_2 are constrained with $\frac{1}{k_2} (1 - \frac{1}{k_1} - \frac{1}{k_2} - \frac{1}{k'_1}) > \frac{2\omega_2^2 \lambda_N^4(\mathcal{L}) \bar{\theta}^2}{(1-2\theta^2 \lambda_N^2(\mathcal{L})) \lambda_{\min}^2(Q_2)}$, $k'_1 \leq -\frac{\lambda_{\min}(Q_2)}{\gamma_1 \epsilon_1^2 \lambda_{\max}^2(\Theta)}$, $k'_2 \leq -\frac{\lambda_{\min}(Q_3)}{\gamma_1 \epsilon_2^2 \lambda_{\max}^2(\Theta)}$, and the event-triggered threshold is satisfied with $\bar{\theta} \in (0, \sqrt{\frac{1}{2\lambda_N^2(\mathcal{L})}})$. Matrices P_1, R and Q_1 are derived from algebraic Riccati equation (ARE): $P_1 A + A^T P_1 - P_1 B R^{-1} B^T P_1 + Q_1 = 0$.

Then, the fault-estimation matrix $K_f = (B^T B)^{-1} B^T F$, the adjacency information-based broadcasting matrix $K_2 = \tau R^{-1} B^T P_1$ with $\tau \geq \frac{1}{2\lambda_2(\mathcal{L})}$, and the positive scalars $\omega_1 = \|P_1 B K_1\|$, $\omega_2 = \|P_1 B K_2\|$, $\omega_3 = \|P_2 B K_1\|$, $\epsilon_1 = \|P_1 D_1\|$, and $\epsilon_2 = \|P_2 D_1\|$.

Thus, for a positive scalar $\sigma^* \in (0, \alpha_1)$, the DoS attack frequency $\mathcal{F}_{\Gamma^a}(t_0, t)$ and the ADT τ_a satisfy

$$\mathcal{F}_{\Gamma^a}(t_0, t) \leq \frac{\sigma^*}{\ln(\zeta \phi)}, \tau_a > \frac{\alpha_1 + \alpha_2}{\alpha_1 - \sigma^*} \quad (19)$$

where $\phi = \max\{\phi_1^{-1} \bar{\phi}_1, \phi_2^{-1} \bar{\phi}_2\}$ and $\zeta = \frac{N}{\gamma_1} \bar{d}_2^2$ with $\bar{\phi}_1 = \lambda_{\max}(P_1)$, $\phi_1 = \lambda_{\min}(P_1)$, $\bar{\phi}_2 = \lambda_{\max}(P_2)$, $\phi_2 = \lambda_{\min}(P_2)$, $\bar{d}_2 = \max_{i=1, \dots, N} \bar{d}_{i2}$, and the consensus control is exponentially realized with the average state consensus error

$$\|e_i(t)\|^2 \leq \mu_\Gamma e^{-\sigma(t-t_0)} \|e_i(t_0)\|^2 \quad (20)$$

where the decay rate σ is given as $\sigma = \alpha_1 - \frac{\alpha_1 + \alpha_2}{\tau_a} - \sigma^*$ and the initial maximum magnitude μ_Γ is determined by

$$\mu_\Gamma = \frac{e^{(\alpha_1 + \alpha_2)\Gamma_0} (\max\{\lambda_{\max}(P_1), \lambda_{\max}(P_2)\} + \eta_\Gamma)}{\min\{\lambda_{\min}(P_1), \lambda_{\min}(P_2)\}} \quad (21)$$

Proof: From Definition 2.1, the total time interval $[t_0, t]$ can be divided into $\Gamma^s(t_0, t)$ (case 1) and $\Gamma^a(t_0, t)$ (case 2) in Fig. 1(b) according to whether DoS attacks occur. In case 1, the event-triggered FTCC mechanism is activated and the DoS attack is sleeping, that is, each event-triggered threshold condition $\|\delta_i(t)\| \leq \theta_i \|\Xi_i(x_{j \in \mathcal{N}_i}^b(t))\|$ holds. In case 2, the event-triggered FTCC mechanism is dormant, and the

DoS attack is activated, that is, the event-triggered threshold condition does not hold.

Case 1: event-triggered FTCC activation and DoS attack sleeping

Consider the time interval $\Gamma^s(t_0, t)$ under which the event-triggered threshold condition $\|\delta_i(t)\| \leq \theta_i \|\Xi_i(x_{j \in \mathcal{N}_i}^b(t))\|$ holds. Firstly, construct a Lyapunov candidate $V_1(e(t)) = e^T(t)(I_N \otimes P_1)e(t)$ with a positive-definite symmetric matrix P_1 . On the basis of the solvable ARE $P_1 A + A^T P_1 - P_1 B R^{-1} B^T P_1 + Q_1 = 0$, the linear matrix inequality (LMI) (16), (17), and $K_2 = \tau R^{-1} B^T P_1$ with $\tau \geq \frac{1}{2\lambda_2(\mathcal{L})}$, the differential of $V_1(e(t))$ with respect to time is obtained as

$$\begin{aligned} \dot{V}_1(e(t)) &= e^T(t)(I_N \otimes (P_1(A - B K_x) + (A - B K_x)^T P_1) \\ &\quad - 2(\mathcal{L} \otimes P_1 B K_2))e(t) + 2e^T(t)(\Theta \otimes P_1 B K_1)\bar{e}(t) \\ &\quad - 2e^T(t)(\mathcal{L} \otimes P_1 B K_2)\delta(t) + 2e^T(t)(\Theta \otimes P_1 D_1)d_1(t) \\ &\leq -\lambda_{\min}(Q_2) \sum_{i=1}^N \tilde{e}_i^T(t)\tilde{e}_i(t) \\ &\quad + \omega_1 \sum_{i=1}^N (\rho_1 \lambda_{\max}^2(\Theta) \tilde{e}_i^T(t)\tilde{e}_i(t) + \rho_1^{-1} \tilde{e}_i^T(t)\tilde{e}_i(t)) \\ &\quad + \omega_2 \sum_{i=1}^N (\rho_2 \lambda_N^2(\mathcal{L}) \tilde{e}_i^T(t)\tilde{e}_i(t) + \rho_2^{-1} \tilde{\delta}_i^T(t)\tilde{\delta}_i(t)) \\ &\quad + \epsilon_1 \sum_{i=1}^N (\bar{\epsilon}_1 \lambda_{\max}^2(\Theta) \tilde{e}_i^T(t)\tilde{e}_i(t) + \bar{\epsilon}_1^{-1} \tilde{d}_{i1}^T(t)\tilde{d}_{i1}(t)) \end{aligned} \quad (22)$$

where $\tilde{e}(t) = \text{col}(\tilde{e}_i(t)) = (\Psi^T \otimes I_{n+q+s_2})\bar{e}(t)$, $\tilde{\delta}(t) = \text{col}(\tilde{\delta}_i(t)) = (\Psi^T \otimes I_n)\delta(t)$, $\tilde{e}(t) = \text{col}(\tilde{e}_i(t)) = (\Psi^T \otimes I_n)e(t)$, $\tilde{d}_1(t) = \text{col}(\tilde{d}_{i1}(t)) = (\Psi^T \otimes I_{s_1})d_1(t)$, $\omega_1 = \|P_1 B K_1\|$, $\omega_2 = \|P_1 B K_2\|$, $\epsilon_1 = \|P_1 D_1\|$, $\rho_1 > 0$, $\rho_2 > 0$, and $\bar{\epsilon}_1 > 0$.

By using the internal positive scalars k_1, k_2 , and k'_1 , it follows that

$$\begin{aligned} \dot{V}_1(e(t)) &\leq -(1 - \frac{1}{k_1} - \frac{1}{k_2} - \frac{1}{k'_1}) \lambda_{\min}(Q_2) \sum_{i=1}^N \tilde{e}_i^T(t)\tilde{e}_i(t) \\ &\quad + \frac{k_1 \omega_1^2 \lambda_{\max}^2(\Theta)}{\lambda_{\min}(Q_2)} \sum_{i=1}^N \tilde{e}_i^T(t)\tilde{e}_i(t) + \frac{k_2 \omega_2^2 \lambda_N^2(\mathcal{L})}{\lambda_{\min}(Q_2)} \sum_{i=1}^N \tilde{\delta}_i^T(t)\tilde{\delta}_i(t) \\ &\quad + \frac{k'_1 \epsilon_1^2 \lambda_{\max}^2(\Theta)}{\lambda_{\min}(Q_2)} \sum_{i=1}^N \tilde{d}_{i1}^T(t)\tilde{d}_{i1}(t) \end{aligned} \quad (23)$$

Since $x^b(t) = \delta(t) + x(t)$ with $x^b(t) = \text{col}(x_{j \in \mathcal{N}_i}^b(t))$, it is derived that $\Xi(x_{j \in \mathcal{N}_i}^b(t)) = -(\mathcal{L} \otimes I_n)(\delta(t) + x(t))$ with $\Xi(x_{j \in \mathcal{N}_i}^b(t)) = \text{col}(\Xi_i(x_{j \in \mathcal{N}_i}^b(t)))$. It follows that

$$\|\Xi(x_{j \in \mathcal{N}_i}^b(t))\| \leq \|\Xi(x_{j \in \mathcal{N}_i}(t))\| + \lambda_N(\mathcal{L})\|\delta(t)\| \quad (24)$$

where $\Xi(x_{j \in \mathcal{N}_i}(t)) = \text{col}(\Xi_i(x_{j \in \mathcal{N}_i}(t)))$ with the distributed adjacency value $\Xi_i(x_{j \in \mathcal{N}_i}(t)) = \sum_{j \in \mathcal{N}_i} (x_j(t) - x_i(t))$.

Then, with $\mathcal{L}\Theta = \Theta\mathcal{L} = \mathcal{L}$ in Theorem 3.1, it follows that

$$\begin{aligned} \|\Xi(x_{j \in \mathcal{N}_i}(t))\|^2 &\leq \lambda_N^2(\mathcal{L})x^T(t)(\Theta^2 \otimes I_n)x(t) = \lambda_N^2(\mathcal{L})e^T(t)e(t) \end{aligned} \quad (25)$$

Combining (24) and (25) yields to $\|\Xi(x_{j \in \mathcal{N}_i}^b(t))\|^2 \leq 2\lambda_N^2(\mathcal{L})(\|e(t)\|^2 + \|\delta(t)\|^2)$. Both $\delta^T(t)\delta(t) \leq \bar{\theta}^2 \|\Xi(x_{j \in \mathcal{N}_i}(t))\|^2$ and $\|\delta(t)\|^2 \leq \frac{2\bar{\theta}^2 \lambda_N^2(\mathcal{L})}{1-2\theta^2 \lambda_N^2(\mathcal{L})} \|e(t)\|^2$ are derived since $\|\delta_i(t)\| \leq \theta_i \|\Xi_i(x_{j \in \mathcal{N}_i}^b(t))\|$, $\bar{\theta} = \max_{i=1, \dots, N} \theta_i \in (0, \sqrt{\frac{1}{2\lambda_N^2(\mathcal{L})}})$.

The first-order time derivative of the complicated actuator faults is calculated as $\dot{f}_i(t) = [f_{i1}^T(t), \dots, f_{iq}^T(t)]^T$ and the second-order derivative is derived as $\ddot{f}_i(t) = -\text{diag}(\epsilon_1, \dots, \epsilon_q)\dot{f}_i(t)$, where $\dot{f}_{is}(t) = -\epsilon_s \dot{f}_{is}(t)$, $s = 1, \dots, q$ with the fault decay rate $\epsilon_s > 0$.

Secondly, consider a Lyapunov candidate $V_2(\bar{e}(t), \dot{f}(t)) = \frac{1}{\gamma_1} \sum_{i=1}^N \bar{e}_i^T(t) \bar{e}_i(t) + \frac{1}{\gamma_2} \sum_{i=1}^N \dot{f}_i^T(t) \dot{f}_i(t)$, where γ_1 and γ_2 are preset positive scalars. The differential of $V_2(\bar{e}(t), \dot{f}_i(t))$ with respect to time is obtained as

$$\begin{aligned} & \dot{V}_2(\bar{e}(t), \dot{f}(t)) \\ & \leq \frac{1}{\gamma_1} \sum_{i=1}^N \bar{e}_i^T(t) (L + L^T + M \bar{D} \bar{D}^T M^T) \bar{e}_i(t) \\ & \quad + \left(\frac{1}{\gamma_1} - \frac{2 \min \epsilon_s}{\gamma_2} \right) \sum_{i=1}^N \dot{f}_i^T(t) \dot{f}_i(t) \\ & \quad + \frac{1}{\gamma_1} \sum_{i=1}^N (d_{i1}^T(t) \dot{d}_{i1}(t) + \dot{d}_{i2}^T(t) \dot{d}_{i2}(t)) \end{aligned} \quad (26)$$

where $\min \epsilon_s = \min_{s=1, \dots, q} \epsilon_s$.

According to the scalar constraints of α_1, k_1, k_2, k'_1 and $\bar{\theta}$, it is given by $(1 - \frac{1}{k_1} - \frac{1}{k_2} - \frac{1}{k'_1}) \lambda_{\min}(Q_2) - \frac{2k_2 \omega_2^2 \lambda_N^4(\mathcal{L}) \bar{\theta}^2}{(1-2\theta^2 \lambda_N^2(\mathcal{L})) \lambda_{\min}(Q_2)} \geq \alpha_1 \lambda_{\max}(P_1)$ with $\frac{1}{k_2} - \frac{1}{k_1 k_2} - \frac{1}{k'_2} - \frac{1}{k'_1 k_2} > \frac{2\omega_2^2 \lambda_N^4(\mathcal{L}) \bar{\theta}^2}{(1-2\theta^2 \lambda_N^2(\mathcal{L})) \lambda_{\min}^2(Q_2)}$. Then, $\frac{k_1 \omega_1^2 \lambda_{\max}^2(\Theta)}{\lambda_{\min}(Q_2)} I_{n+q+s_2} + \frac{1}{\gamma_1} (L + L^T + M \bar{D} \bar{D}^T M^T) + \frac{\alpha_1}{\gamma_1} I_{n+q+s_2} < 0$ is obtained from (17) with $L + L^T + M \bar{D} \bar{D}^T M^T < -\eta_{\alpha_1} I_{n+q+s_2}$.

Ultimately, construct the Lyapunov candidate $V_{tri}(t) = V_1(e(t)) + V_2(\bar{e}(t), \dot{f}(t))$ in the event-triggered activation period as shown in Fig. 1(b), it then follows that

$$\begin{aligned} & \dot{V}_{tri}(t) \\ & \leq -\left(1 - \frac{1}{k_1} - \frac{1}{k_2} - \frac{1}{k'_1}\right) \lambda_{\min}(Q_2) \sum_{i=1}^N \bar{e}_i^T(t) \bar{e}_i(t) \\ & \quad + \sum_{i=1}^N \bar{e}_i^T(t) \left(\frac{k_1 \omega_1^2 \lambda_{\max}^2(\Theta)}{\lambda_{\min}(Q_2)} I_{n+q+s_2} + \frac{1}{\gamma_1} (L + L^T + M \bar{D} \right. \\ & \quad \times \bar{D}^T M^T) \bar{e}_i(t) + \frac{2k_2 \omega_2^2 \lambda_N^4(\mathcal{L}) \bar{\theta}^2}{(1-2\theta^2 \lambda_N^2(\mathcal{L})) \lambda_{\min}(Q_2)} \sum_{i=1}^N \bar{e}_i^T(t) \bar{e}_i(t) \\ & \quad \left. + \left(\frac{1}{\gamma_1} - \frac{2 \min \epsilon_s}{\gamma_2} \right) \sum_{i=1}^N \dot{f}_i^T(t) \dot{f}_i(t) + \frac{1}{\gamma_1} \sum_{i=1}^N \dot{d}_{i2}^T(t) \dot{d}_{i2}(t) \right) \\ & \quad + \left(\frac{1}{\gamma_1} + \frac{k'_1 \epsilon_1^2 \lambda_{\max}^2(\Theta)}{\lambda_{\min}(Q_2)} \right) \sum_{i=1}^N d_{i1}^T(t) \dot{d}_{i1}(t) \\ & \leq -\alpha_1 \lambda_{\max}(P_1) \sum_{i=1}^N \bar{e}_i^T(t) \bar{e}_i(t) - \frac{\alpha_1}{\gamma_1} \sum_{i=1}^N \bar{e}_i^T(t) \bar{e}_i(t) \\ & \quad + \left(\frac{1}{\gamma_1} - \frac{2 \min \epsilon_s}{\gamma_2} \right) \sum_{i=1}^N \dot{f}_i^T(t) \dot{f}_i(t) + \frac{1}{\gamma_1} \sum_{i=1}^N \dot{d}_{i2}^T(t) \dot{d}_{i2}(t) \\ & \quad + \left(\frac{1}{\gamma_1} + \frac{k'_1 \epsilon_1^2 \lambda_{\max}^2(\Theta)}{\lambda_{\min}(Q_2)} \right) \sum_{i=1}^N d_{i1}^T(t) \dot{d}_{i1}(t) \\ & \leq -\alpha_1 V_{tri}(t) + \left(\frac{\alpha_1}{\gamma_2} + \frac{1}{\gamma_1} - \frac{2 \min \epsilon_s}{\gamma_2} \right) \sum_{i=1}^N \dot{f}_i^T(t) \dot{f}_i(t) \\ & \quad + \frac{1}{\gamma_1} \sum_{i=1}^N \dot{d}_{i2}^T(t) \dot{d}_{i2}(t) \end{aligned} \quad (27)$$

where $k'_1 \leq -\frac{\lambda_{\min}(Q_2)}{\gamma_1 \epsilon_1^2 \lambda_{\max}^2(\Theta)}$ is set manually.

According to $\frac{\gamma_2}{\gamma_1} \leq \min\{2\epsilon_{\text{inc}} - \alpha_1, 2\epsilon_{\text{inc}} + \alpha_2\}$ and $\min \epsilon_s \geq \epsilon_{\text{inc}}$ in Assumption 2.1, $\alpha_1 + \frac{\gamma_2}{\gamma_1} \leq 2\epsilon_{\text{inc}}$ is derived. Then, it is obtained that $\frac{\alpha_1}{\gamma_2} + \frac{1}{\gamma_1} - \frac{2 \min \epsilon_s}{\gamma_2} \leq 0$. Therefore, the proof of $\dot{V}_{tri}(t) \leq -\alpha_1 V_{tri}(t) + \frac{1}{\gamma_1} \sum_{i=1}^N \dot{d}_{i2}^T(t) \dot{d}_{i2}(t)$ is completed.

Case 2: event-triggered FTCC sleeping and DoS attack activation

Consider the time interval $\Gamma^a(t_0, t)$ under which the event-triggered threshold condition does not necessarily hold. For the event-triggered FTCC sleeping and DoS attack activation case, the FTCC design of each agent is modified as $u_i(t) = -K_1 \hat{x}_1(t)$ without the adjacency broadcasting information $\Xi_i(x_{j \in \mathcal{N}_i}^b(t))$. Accordingly, the corresponding average state consensus error systems are modified as $\dot{e}(t) = (I_N \otimes (A - BK_x))e(t) + (\Theta \otimes BK_1)\bar{e}(t) + (\Theta \otimes D_1)d_1(t)$ without the event-triggered error.

Firstly, construct a Lyapunov candidate $V_3(e(t)) = e^T(t)(I_N \otimes P_2)e(t)$ with a positive-definite symmetric matrix P_2 . On the basis of LMI $P_2 A + A^T P_2 - P_2 B K_x - K_x^T B^T P_2 +$

$Q_3 < 0$ in (18), the mathematical representation of the derivative of $V_3(e(t))$ is given as

$$\begin{aligned} \dot{V}_3(e(t)) & \leq -\left(1 - \frac{1}{k_3} - \frac{1}{k'_2}\right) \lambda_{\min}(Q_3) \sum_{i=1}^N \bar{e}_i^T(t) \bar{e}_i(t) \\ & \quad + \frac{k_3 \omega_3^2 \lambda_{\max}^2(\Theta)}{\lambda_{\min}(Q_3)} \bar{e}^T(t) \bar{e}(t) + \frac{k'_2 \epsilon_2^2 \lambda_{\max}^2(\Theta)}{\lambda_{\min}(Q_3)} \bar{d}_1^T(t) \bar{d}_1(t) \end{aligned} \quad (28)$$

where $\omega_3 = \|P_2 B K_1\|$, $\epsilon_2 = \|P_2 D_1\|$, and k_3, k'_2 are positive scalars.

Secondly, consider $V_{tri}(t) = V_3(e(t)) + V_2(\bar{e}(t), \dot{f}(t))$ in event-triggered sleeping period in Fig. 1(b). On the basis of the inequality constraint (17), it is derived as $\frac{k_3 \omega_3^2 \lambda_{\max}^2(\Theta)}{\lambda_{\min}(Q_3)} I_{n+q+s_2} + \frac{1}{\gamma_1} (L + L^T + M \bar{D} \bar{D}^T M^T) - \frac{\alpha_2}{\gamma_1} I_{n+q+s_2} < 0$ with $L + L^T + M \bar{D} \bar{D}^T M^T < -\eta_{\alpha_2} I_{n+q+s_2}$. Then, with the scalar constraints of α_2, k_3 , and k'_2 , $(1 - \frac{1}{k_3} - \frac{1}{k'_2}) \lambda_{\min}(Q_3) \geq -\alpha_2 \lambda_{\min}(P_2)$ is derived. The first-order time derivative of $V_{tri}(t)$ is derived as

$$\begin{aligned} & \dot{V}_{tri}(t) \\ & \leq -\left(1 - \frac{1}{k_3} - \frac{1}{k'_2}\right) \lambda_{\min}(Q_3) \bar{e}^T(t) \bar{e}(t) + \frac{k_3 \omega_3^2 \lambda_{\max}^2(\Theta) \bar{e}^T(t) \bar{e}(t)}{\lambda_{\min}(Q_3)} \\ & \quad + \frac{1}{\gamma_1} \sum_{i=1}^N \bar{e}_i^T(t) (L + L^T + M \bar{D} \bar{D}^T M^T) \bar{e}_i(t) \\ & \quad + \left(\frac{1}{\gamma_1} - \frac{2 \min \epsilon_s}{\gamma_2} \right) \sum_{i=1}^N \dot{f}_i^T(t) \dot{f}_i(t) + \frac{1}{\gamma_1} \sum_{i=1}^N \dot{d}_{i2}^T(t) \dot{d}_{i2}(t) \\ & \quad + \left(\frac{1}{\gamma_1} + \frac{k'_2 \epsilon_2^2 \lambda_{\max}^2(\Theta)}{\lambda_{\min}(Q_3)} \right) \sum_{i=1}^N d_{i1}^T(t) \dot{d}_{i1}(t) \\ & \leq \alpha_2 \lambda_{\min}(P_2) \sum_{i=1}^N \bar{e}_i^T(t) \bar{e}_i(t) + \frac{\alpha_2}{\gamma_1} \bar{e}^T(t) \bar{e}(t) \\ & \quad + \left(\frac{1}{\gamma_1} - \frac{2 \min \epsilon_s}{\gamma_2} \right) \sum_{i=1}^N \dot{f}_i^T(t) \dot{f}_i(t) + \frac{1}{\gamma_1} \sum_{i=1}^N \dot{d}_{i2}^T(t) \dot{d}_{i2}(t) \\ & \quad + \left(\frac{1}{\gamma_1} + \frac{k'_2 \epsilon_2^2 \lambda_{\max}^2(\Theta)}{\lambda_{\min}(Q_3)} \right) \sum_{i=1}^N d_{i1}^T(t) \dot{d}_{i1}(t) \\ & \leq \alpha_2 V_{tri}(t) + \left(\frac{1}{\gamma_1} - \frac{\alpha_2}{\gamma_2} - \frac{2 \min \epsilon_s}{\gamma_2} \right) \sum_{i=1}^N \dot{f}_i^T(t) \dot{f}_i(t) \\ & \quad + \frac{1}{\gamma_1} \sum_{i=1}^N \dot{d}_{i2}^T(t) \dot{d}_{i2}(t) \end{aligned} \quad (29)$$

where $k'_2 \leq -\frac{\lambda_{\min}(Q_3)}{\gamma_1 \epsilon_2^2 \lambda_{\max}^2(\Theta)}$ is set manually.

According to the same condition of $\frac{\gamma_2}{\gamma_1}$ and $\min \epsilon_s \geq \epsilon_{\text{inc}}$ in Assumption 2.1, it also follows that $\frac{1}{\gamma_1} - \frac{\alpha_2}{\gamma_2} - \frac{2 \min \epsilon_s}{\gamma_2} \leq 0$. Thus, $\dot{V}_{tri}(t) \leq \alpha_2 V_{tri}(t) + \frac{1}{\gamma_1} \sum_{i=1}^N \dot{d}_{i2}^T(t) \dot{d}_{i2}(t)$ is proved.

Integrating both sides of $\dot{V}_{tri}(t) \leq -\alpha_1 V_{tri}(t) + \frac{\dot{d}_2^T(t) \dot{d}_2(t)}{\gamma_1}$ and $\dot{V}_{tri}(t) \leq \alpha_2 V_{tri}(t) + \frac{\dot{d}_2^T(t) \dot{d}_2(t)}{\gamma_1}$ over $[t_k, t_{k+1})$ yields to

$$\begin{cases} V_{tri}(t) \leq \zeta e^{-\alpha_1(t-t_k)} V_{tri}(t_k) + \frac{\zeta}{\alpha_1} \\ V_{tri}(t) \leq \zeta e^{\alpha_2(t-t_k)} V_{tri}(t_k) - \frac{\zeta}{\alpha_2} \end{cases} \quad (30)$$

where $\zeta = \frac{N}{\gamma_1} \bar{d}_2^2$ with $\bar{d}_2 = \max_{i=1, \dots, N} \bar{d}_{i2}$.

Denote the piecewise Lyapunov candidate $V(t) = V_{tri}(t)$ and $V_{tri}(t)$ is activated when $t \in [t_{r-1}^a + \Delta_{r-1}^a, t_r^a)$, and further define $V(t) = V_{tri}(t)$ and $V_{tri}(t)$ is activated in $[t_r^a, t_r^a + \Delta_r^a)$. Integrating both sides over $t \in [t_{r-1}^a + \Delta_{r-1}^a, t_r^a + \Delta_r^a)$,

$$V(t) \leq \begin{cases} \zeta e^{-\alpha_1(t-t_{r-1}^a - \Delta_{r-1}^a)} V_{tri}(t_{r-1}^a + \Delta_{r-1}^a) \\ \zeta e^{\alpha_2(t-t_r^a)} V_{tri}(t_r^a) \end{cases} \quad (31)$$

Notable, $\phi_1 V_1(e(t)) \leq \sum_{i=1}^N e_i^T(t) P_1 e_i(t) \leq \bar{\phi}_1 V_1(e(t))$ and $\phi_2 V_3(e(t)) \leq \sum_{i=1}^N e_i^T(t) P_2 e_i(t) \leq \bar{\phi}_2 V_3(e(t))$, where $\bar{\phi}_1 = \lambda_{\max}(P_1)$, $\phi_1 = \lambda_{\min}(P_1)$, $\bar{\phi}_2 = \lambda_{\max}(P_2)$ and $\phi_2 = \lambda_{\min}(P_2)$. At each event-triggering instant $t_{k_j}^i$, it is derived that $V_{tri}(t_{k_i}^i) \leq \frac{\bar{\phi}_1}{\phi_1} V_{tri}(t_{k_i}^i)$ and $V_{tri}(t_{k_i}^i) \leq \frac{\phi_2}{\bar{\phi}_2} V_{tri}(t_{k_i}^i)$.

Then, for $t \in [t_{r-1}^a + \Delta_{r-1}^a, t_r^a]$, $N_{\Gamma^a}(t_0, t) = r$ is derived and the Lyapunov form $V_{tri}(t)$ is given as

$$\begin{aligned} V_{tri}(t) &\leq \zeta \frac{\bar{\phi}_1}{\phi_1} e^{-\alpha_1(t-t_{r-1}^a - \Delta_{r-1}^a)} V_{tri}(t_{r-1}^a + \Delta_{r-1}^a) \\ &\leq \frac{\zeta^2 \bar{\phi}_1}{\phi_1} e^{-\alpha_1(t-t_{r-1}^a - \Delta_{r-1}^a)} [e^{\alpha_2(t-t_{r-2}^a - \Delta_{r-2}^a)} V_{tri}(t_{r-2}^a + \Delta_{r-2}^a)] \\ &\leq \frac{\zeta^2 \bar{\phi}_1 \bar{\phi}_2}{\phi_1 \phi_2} e^{-\alpha_1(t-t_{r-1}^a - \Delta_{r-1}^a)} e^{\alpha_2(t-t_{r-2}^a - \Delta_{r-2}^a)} V_{tri}(t_{r-2}^a + \Delta_{r-2}^a) \\ &\leq \dots \leq \zeta^r \phi^r e^{-\alpha_1 |\Gamma^s(t_0, t)|} e^{\alpha_2 |\Gamma^a(t_0, t)|} V_{tri}(t_0) \\ &= e^{\ln(\zeta \phi) N_{\Gamma^a}(t_0, t)} e^{-\alpha_1 |\Gamma^s(t_0, t)| + \alpha_2 |\Gamma^a(t_0, t)|} V_{tri}(t_0) \end{aligned} \quad (32)$$

where $\phi = \max\{\frac{\phi_1^{-1} \bar{\phi}_1}{\phi_1}, \frac{\phi_2^{-1} \bar{\phi}_2}{\phi_2}\}$.

Next, for $t \in [t_r^a, t_r^a + \Delta_r^a]$, $N_{\Gamma^a}(t_0, t) = r + 1$ is obtained and the Lyapunov form is given by

$$\begin{aligned} V_{tri}(t) &\leq \zeta \frac{\bar{\phi}_2}{\phi_2} e^{\alpha_2(t-t_r^a)} V_{tri}(t_r^a) \\ &\leq \frac{\zeta^2 \bar{\phi}_2}{\phi_2} e^{\alpha_2(t-t_r^a)} [e^{-\alpha_1(t-t_{r-1}^a - \Delta_{r-1}^a)} V_{tri}(t_{r-1}^a + \Delta_{r-1}^a)] \\ &\leq \frac{\zeta^2 \bar{\phi}_2 \bar{\phi}_1}{\phi_2 \phi_1} e^{\alpha_2(t-t_r^a)} e^{-\alpha_1(t-t_{r-1}^a - \Delta_{r-1}^a)} V_{tri}(t_{r-1}^a + \Delta_{r-1}^a) \\ &\leq \dots \leq \zeta^{r+1} \phi^{r+1} e^{-\alpha_1 |\Gamma^s(t_0, t)|} e^{\alpha_2 |\Gamma^a(t_0, t)|} V_{tri}(t_0) \\ &= e^{\ln(\zeta \phi) N_{\Gamma^a}(t_0, t)} e^{-\alpha_1 |\Gamma^s(t_0, t)| + \alpha_2 |\Gamma^a(t_0, t)|} V_{tri}(t_0) \end{aligned} \quad (33)$$

From Definitions 2.1-2.3, $|\Gamma^s(t_0, t)| = t - t_0 - |\Gamma^a(t_0, t)|$ and $\Gamma^a(t_0, t) \leq \Gamma_0 + \frac{t-t_0}{\tau_a}$ are given by the ADT τ_a and chattering bound Γ_0 . According to the inequality constraints of DoS attack frequency $\mathcal{F}_{\Gamma^a}(t_0, t) = \frac{N_{\Gamma^a}(t_0, t)}{t-t_0} \leq \frac{\sigma^*}{\ln(\zeta \phi)}$ and ADT $\tau_a > \frac{\alpha_1 + \alpha_2}{\alpha_1 - \sigma^*}$ in (19), for $\forall t \geq t_0$, it follows that

$$\begin{aligned} V(t) &\leq e^{(\alpha_1 + \alpha_2) \Gamma_0 + \ln(\zeta \phi) N_{\Gamma^a}(t_0, t) + (\frac{\alpha_1 + \alpha_2}{\tau_a} - \alpha_1)(t-t_0)} V(t_0) \\ &\leq e^{(\alpha_1 + \alpha_2) \Gamma_0 - \alpha_1(t-t_0) + \frac{\alpha_1 + \alpha_2}{\tau_a}(t-t_0) + \sigma^*(t-t_0)} V(t_0) \\ &= e^{(\alpha_1 + \alpha_2) \Gamma_0} e^{-\sigma(t-t_0)} V(t_0) \end{aligned} \quad (34)$$

where $\sigma = \alpha_1 - \frac{\alpha_1 + \alpha_2}{\tau_a} - \sigma^* > 0$ with $\sigma^* \in (0, \alpha_1)$.

From the definition of $V_{tri}(t)$ and $V_{tri}(t)$, it is derived that $V(t) \geq \min\{\lambda_{\min}(P_1), \lambda_{\min}(P_2)\} \|e_i(t)\|^2$, and the expression with t_0 is derived as

$$\begin{aligned} V(t_0) &\leq (\max\{\lambda_{\max}(P_1), \lambda_{\max}(P_2)\} \\ &\quad + \frac{\max_{i=1, \dots, N} (\frac{1}{\gamma_1} \|\bar{e}_i(t_0)\|^2 + \frac{1}{\gamma_2} \|\bar{f}_i(t_0)\|^2)}{\min_{i=1, \dots, N} \|e_i(t_0)\|^2}) \|e_i(t_0)\|^2 \end{aligned} \quad (35)$$

Denote $\Lambda_{\Gamma} = \max\{\lambda_{\max}(P_1), \lambda_{\max}(P_2)\} + \eta_{\Gamma}$ with the appropriate positive scalar η_{Γ} , it is finally given by

$$\begin{aligned} \|e_i(t)\|^2 &\leq \frac{V(t)}{\min\{\lambda_{\min}(P_1), \lambda_{\min}(P_2)\}} \\ &\leq \frac{e^{(\alpha_1 + \alpha_2) \Gamma_0} e^{-\sigma(t-t_0)}}{\min\{\lambda_{\min}(P_1), \lambda_{\min}(P_2)\}} V(t_0) \leq \mu_{\Gamma} e^{-\sigma(t-t_0)} \|e_i(t_0)\|^2 \end{aligned} \quad (36)$$

where $\mu_{\Gamma} = \frac{e^{(\alpha_1 + \alpha_2) \Gamma_0} \Lambda_{\Gamma}}{\min\{\lambda_{\min}(P_1), \lambda_{\min}(P_2)\}}$.

Therefore, the inequality $\|e_i(t)\|^2 \leq \mu_{\Gamma} e^{-\sigma(t-t_0)} \|e_i(t_0)\|^2$ in (36) implies that $\|e_i(t)\|^2 \rightarrow \|e_i(t_0)\|^2$, $x_i(t) \rightarrow \hat{x}_i(t)$, $f_i(t) \rightarrow \hat{f}_i(t)$ and $x_i(t) \rightarrow \frac{1}{N} \sum_{i=1}^N x_i(t_0)$ as $t \rightarrow +\infty$ when the chattering bound Γ_0 and ADT τ_a are satisfied in (19), i.e., $\mu_{\Gamma} > 0$ and $\sigma > 0$. Moreover, exponential achievement of the average state consensus objective in MASs under both actuator faults and aperiodic DoS attacks is attained through the distributed event-triggered FTCC scheme.

Remark 3.2: The calculation of the ALO-CLE-based decentralized FE and RBS-OLE-based distributed event-triggered FTCC schemes is succinctly outlined in Algorithm 1.

Algorithm 1 Distributed event-triggered FTCC solution.

Input:

- The set of system matrices: $\{A, B, C, F, D_1, D_2\}$.
- The set of graph matrix: $\{\mathcal{L}\}$.
- The set of preset scalars: $\{\gamma_1, \gamma_2, \underline{\epsilon}_{\text{inc}}, \eta_{\Gamma}\}$.

Output:

- The set of designed matrices: $\{L, G, J, H, K_1, K_2\}$.
- 1: Solving an ARE: $P_1 A + A^T P_1 - P_1 B R^{-1} B^T P_1 + Q_1 = 0$ to obtain the positive-definite symmetric matrix P_1 and the positive-definite matrices R and Q_1 .
 - 2: Solving an LMI: $-Q_1 - P_1 B K_x - K_x^T B^T P_1 + Q_2 < 0$ to get the positive-definite matrix Q_2 and matrix K_x .
 - 3: Solving an LMI: $P_2 A + A^T P_2 - P_2 B K_x - K_x^T B^T P_2 + Q_3 < 0$ to derive the positive-definite symmetric matrix P_2 and the positive-definite matrix Q_3 .
 - 4: Solving the following LMI:

$$\begin{bmatrix} \min\{\eta_{\alpha_1}, \eta_{\alpha_2}\} + \Pi + \bar{D} \bar{D}^T & H \bar{C} \bar{D} \\ \star & -I_q \end{bmatrix} < 0 \quad (37)$$

to obtain the implicit matrices H and J_1 in (17) with help of the inter matrix $\Pi = \bar{A} + \bar{A}^T - H \bar{C} \bar{A} - \bar{A}^T \bar{C}^T H^T - J_1 \bar{C} - \bar{C}^T J_1^T + \bar{D} \bar{D}^T \bar{C}^T H^T + H \bar{C} \bar{D} \bar{D}^T$.

- 5: **return** The ALO-CLE matrices $L = (I_{n+q+s_2} - H \bar{C}) \bar{A} - J_1 \bar{C}$, $G = (I_{n+q+s_2} - H \bar{C}) \bar{B}$, $J = J_1 + ((I_{n+q+s_2} - H \bar{C}) \bar{A} - J_1 \bar{C}) H$, the fault-estimation matrix $K_f = (B^T B)^{-1} B^T F$, and the broadcasting matrix $K_2 = \tau R^{-1} B^T P_1$ with $\tau \geq \frac{1}{2\lambda_2(L)}$.
-

Remark 3.3: On the basis of the hybrid event-triggered control mechanism [31], Zeno phenomenon does not exhibit with the determination of the following updated control sequence at each event-triggered instant $\{t_{k_i}^i\}_{k_i \in \mathbb{N}}$,

$$t_{k_i+1}^i = \begin{cases} t_{k_i}^i + \chi_i, & \text{if } k_i \in \{(i, k_i) \in \mathcal{V} \times \mathbb{N} \mid t_{k_i}^i \in \cup_{r \in \mathbb{N}} \Gamma_r^a\} \\ t_{k_i}^i + \Delta_{k_i}^z, & \text{otherwise} \end{cases} \quad (38)$$

where the interexecution interval is denoted as $\Delta_{k_i}^z = \max\{\inf_{t > t_{k_i}^i} \{t - t_{k_i}^i \mid \|\delta_i(t)\| = \theta_i \mid \Xi_i(x_{j \in \mathcal{N}_i}^b(t))\}, v_i\}$ with the preset positive scalars χ_i and v_i .

Hence, the event-triggered sleeping interval is denoted as $\cup_{r \in \mathbb{N}} [t_r^a, t_r^a + \Delta_r^a + \Delta_r^z]$. Zeno behavior exclusion case is shown in Fig. 1(c) by proving that there are different positive upper bounds $\sup_{(i, k_i, r)} t_{k_i+1}^i - t_{k_i}^i \leq \Delta_r^z$ corresponding to the relative adjacency broadcasting RBS-OLE.

Furthermore, compared with the sampled-data-based event-triggered [30] and adaptive self-triggered [31], [35] strategies, a basically constant threshold-based static event-triggered mechanism is used to effectively utilize the distributed adjacency broadcasting value $\Xi_i(x_{j \in \mathcal{N}_i}^b(t))$ and the latest triggering state value $x_i^b(t)$, so as to simply update the event triggers located in the sleeping intervals of DoS attacks. The problem of confusing the dynamics of dynamic event-triggered mechanism with the intermittence of DoS attacks without effective discrimination is avoided.

Remark 3.4: (i) Compared with the existing adaptive distributed observers for estimating system matrix and exosystem state [24], fixed-time observers for assessing faults and

disturbances [17], and link-based estimators for evaluating inter-agent state [34], an ALO-CLE-based strategy is seldom considered to construct unmeasurable information of each local agent from FE system to FTCC system. Scheduling the updated control sequence $\{t_{k_i}^i\}_{k_i \in \mathbb{N}}$ in a novel RBS-OLE-based FTCC design and information interaction under DoS attack sequence $\{t_r^a\}_{r \in \mathbb{N}}$ is considered without requiring any solvable fault parameters or preset fault detection and diagnosis mechanism [18]. (ii) Unlike state-feedback control via adaptive mechanism [14], [26], limited output-feedback strategy [19] or impulsive control [21], [22], the proposed FTCC protocol, which depends on the offset item $-K_1 \hat{x}_i(t)$ and the adjacency broadcasting item $K_2 \Xi_i(x_{j \in \mathcal{N}_i}^b(t))$ in this study, can be utilized together with event-triggered strategy in a distributed manner to eliminate continuous monitoring of state measurement errors and avoid high-precision measurement equipments. This distributed mode with communication cost advantage is user-friendly in that there exists a structured low-complexity solution and streamlined non-nested logicity of the algorithm implementation.

Remark 3.5: One advantage is that for the special case of DoS attacks occurring at the triggering time instants, the distributed FTCC is modified as $u_i(t) = -K_1 \hat{x}_i(t) - K_2 \sum_{j \in \mathcal{N}_i} a_{ij} x_j^b(t_{-1}^i)$. One constraint is the tradeoff between the average consensus exponential convergence attenuation rates α_1 and α_2 , the uniform upper bound on the attack frequency $\mathcal{F}_{\Gamma^a}(t_0, t)$ and the lower bound on the ADT τ_a of aperiodic DoS attacks. It is revealed that under sufficient conditions of attack frequency and ADT, the MASs attacked by DoS attacks achieve consensus exponentially by the proposed distributed event-triggered FTCC algorithm with anti-attack performance.

IV. SIMULATION RESULTS

The aim of this section is to demonstrate the effectiveness of the distributed event-triggered FTCC in countering DoS attacks and complicated abrupt and incipient faults, through the use of six single-link manipulators with revolute joints.

The mechanical behavior of the single-link manipulator with flexible joints actuated by a DC motor is outlined as [30]:

$$\begin{cases} \dot{\theta}_{mi} = \omega_{mi} \\ \dot{\omega}_{mi} = \frac{k_s}{J_m} (\theta_{li} - \theta_{mi}) - \frac{l_{link}}{J_m} \omega_{mi} + \frac{k_\tau}{J_m} u_i \\ \dot{\theta}_{li} = \omega_{li} \\ \dot{\omega}_{li} = -\frac{\eta k_s}{J_l} (\theta_{li} - \theta_{mi}) - \frac{\eta \mathcal{M} g h}{J_l} \sin(\theta_{li}) \end{cases} \quad (39)$$

where $\theta_{mi}, \omega_{mi}, \theta_{li}$ and ω_{li} represent the angular rotation of the motor, the angular velocity of the motor, the angular position of the link and the angular velocity of the link, respectively. The physical meanings and values of the parameters are shown in Table I. The corresponding system matrices A and B are denoted in the following form with the small disturbance principle $\sin(\theta_{li}) \cong \theta_{li}$,

$$A = \begin{bmatrix} 0 & 1 & 0 & 0 \\ -\frac{k_s}{J_m} & -\frac{l_{link}}{J_m} & \frac{k_s}{J_m} & 0 \\ 0 & 0 & 0 & 1 \\ -\frac{\eta k_s}{J_l} & 0 & \frac{\eta k_s}{J_l} & -\frac{\eta \mathcal{M} g h}{J_l} \end{bmatrix}, B = \begin{bmatrix} 0 \\ \frac{k_\tau}{J_m} \\ 0 \\ 0 \end{bmatrix} \quad (40)$$

The total activation duration of DoS attacks is denoted as $t \in [0s, 2s] \cup [4s, 6s] \cup [29s, 32s] \cup [49s, 52s] \cup [58s, 61s] \cup [75s, 77s] \cup [81s, 83s]$ for Case I (*short-term DoS interval*). The total activation duration of DoS attacks is denoted as $t \in [3s, 6s] \cup [19s, 22s] \cup [31s, 37s] \cup [46s, 48s] \cup [68s, 73s]$ for Case II (*long-term DoS interval*). The complicated abrupt and incipient faults $f_i(t), i = 1, \dots, 6$ in control inputs for Case I and Case II are modeled as:

Case I (short-term DoS interval):

$$\begin{aligned} f_1(t) &= 1 - e^{-0.5(t-80)} \text{rad}, \\ f_2(t) &= \begin{cases} 0.2(1 - e^{-0.5(t-20)}) \text{rad}, & 20s \leq t \leq 80s \\ 0.5(1 - e^{-0.05(t-80)}) \text{rad}, & t > 80s \end{cases} \\ f_3(t) &= 0.5(1 - e^{-0.03t}) \text{rad}, f_4 = f_5 = f_6 = 0 \text{rad} \end{aligned} \quad (41)$$

Case II (long-term DoS interval):

$$\begin{aligned} f_1(t) &= \begin{cases} 0.5(1 - e^{-0.08(t-30)}) \text{rad}, & 30s \leq t \leq 60s \\ 1.2(1 - e^{-0.3(t-60)}) \text{rad}, & t > 60s \end{cases} \\ f_2(t) &= \begin{cases} 0.5(1 - e^{-0.05(t-30)}) \text{rad}, & 30s \leq t \leq 40s \\ 0.3(1 - e^{-0.03(t-40)}) \text{rad}, & 40s \leq t \leq 60s \\ 1 - e^{-0.6(t-60)} \text{rad}, & t > 60s \end{cases} \\ f_3(t) &= 0.2(1 - e^{-0.05t}) \text{rad}, f_4(t) = 0 \text{rad}, \\ f_5(t) &= 0.6(1 - e^{-0.05(t-40)}) \text{rad}, f_6(t) = 0 \text{rad} \end{aligned} \quad (42)$$

TABLE I
THE PHYSICAL CHARACTERISTICS OF SINGLE-LINK MANIPULATOR [30].

Parameter	Physical meaning	Value/Unit
J_m	inertia of the motor	0.0037kg.m ²
J_l	inertia of the link	0.0093kg.m ²
k_s	torsional spring constant	0.18Nm/rad
k_τ	amplifier gain	0.08Nm/V
η	transformation coefficient	0.1
l_{link}	length of the link	0.31m
h	center of gravity height	0.015m
\mathcal{M}	point mass of the arm	0.139kg

To prove the feasibility of the distributed event-triggered FTCC algorithm in Theorems 3.2, simulation parameters are set as $\gamma_1 = 10.48, \gamma_2 = 0.02, \alpha_1 = 0.0075, \alpha_2 = 0.048, k_1 = 1.85, k_2 = 3.74, k_3 = 0.7, \eta_\Gamma = 1.25$ and $\tau = 0.72$. The maximum and minimum boundaries of the incipient actuator fault in the manipulator are preset as $\bar{\epsilon}_{inc} = 0.1$ and $\underline{\epsilon}_{inc} = 0.005$. The initial angular rotation and angular velocity of the motor, and the angular position and angular velocity of the link are set as 0.25rad, 0.5rad.s⁻¹, 0.1rad, and 0.1rad.s⁻¹, respectively. The event-triggered threshold is constrained within (0, 0.138). The topology under DoS attacks for short-term DoS interval in Case I is depicted in Fig. 3, where the first manipulator encounters an unexpected actuator fault ($T_1 = 80s$), the second one fails with the complicated incipient and abrupt actuator fault ($T_2 = 20s, 80s$), and the third one fails with the initially existing incipient actuator fault. Furthermore, the topology under DoS attacks for long-term DoS interval in Case II is shown in Fig. 3, wherein the first and second manipulators suffer from the complicated incipient and abrupt actuator faults ($T_1 = 30s, 60s$ and $T_2 = 30s, 40s, 60s$), and the third and fifth manipulators exhibit the incipient actuator faults at each fault event moment, i.e., $T_3 = 0s$ and $T_5 = 40s$.

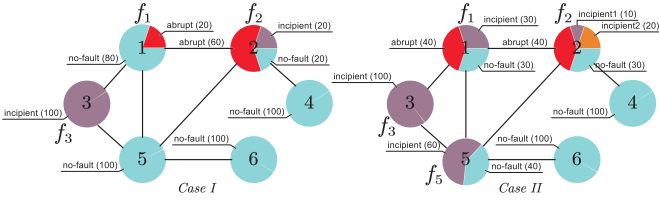


Fig. 3. The topologies under DoS attacks (Case I: short-term DoS interval and Case II: long-term DoS interval).

In the scenario of the aperiodic DoS attacks in networked hierarchy and complicated abrupt and incipient actuator faults in physical hierarchy, the results in Figs. 4-7 under short-term DoS interval (case I) and in Figs. 8-11 under long-term DoS interval (case II) confirm the effectiveness of the distributed event-triggered FTCC schemes in Theorems 3.1 and 3.2. Compared with the switching mechanism-based FTCC technique [15], the average consensus errors of the angular rotations $\theta_{mi} - \sum_{i=1}^6 \theta_{mi}$ and the angular velocities $\omega_{mi} - \sum_{i=1}^6 \omega_{mi}$, $i = 1, \dots, 6$ of each motor in Case I in Fig. 4 and Fig. 5, and the average consensus errors of the angular positions $\theta_{li} - \sum_{i=1}^6 \theta_{li}$ and the angular velocities $\omega_{li} - \sum_{i=1}^6 \omega_{li}$, $i = 1, \dots, 6$ of each link in Case I in Fig. 6 and Fig. 7 show smaller convergence amplitude and faster convergence speed via the proposed attack frequency and ADT-based FTCC technique. The abrupt actuator fault of the first manipulator occurs in 80s and causes the average consensus errors to jump up and down. The tiny and abrupt fault of the second manipulator occurs in 20s and leads to slight varying of consensus errors. In the third manipulator, the incipient actuator fault exists in the early stage, and the long-term error change is not obvious. The consensus error signal of the fifth manipulator also fluctuates slightly for a long period due to the interconnection with manipulators 1, 2 and 3. Due to the short-term interval of DoS attacks in Case I, a convergence with slight oscillations of varying amplitudes is formed, and finally the exponential consensus control objective is accomplished with the distributed event-triggered FTCC provided that the DoS attack frequency and ADT always hold.

Comparative results of the average consensus errors of the angular rotations and angular velocities of each motor in Fig. 8 and Fig. 9 and the angular positions and angular velocities of each link in Fig. 10 and Fig. 11 under long-term DoS interval in Case II are depicted. Both the first and second manipulators have abrupt actuator faults in 60s and produce large amplitude excitation error signals. The incipient actuator faults with different amplitudes fail on the second manipulator in 30s and 40s, the long-standing incipient faults act on the third manipulator, and the tiny actuator faults occur on the fifth manipulator in 40s. Compared with the short-term DoS attacks, because the DoS attack frequency and ADT index does not always satisfied, the average consensus errors oscillate violently in the long-term interval of DoS attacks, especially after the wider widths [31s, 37s] and [68s, 73s]. Furthermore, the controller response curves under short-term DoS interval in Case I and long-term DoS interval in Case II are shown in

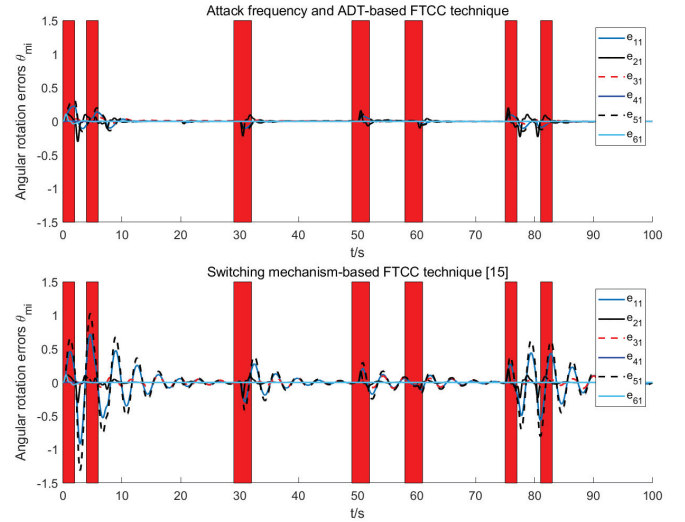


Fig. 4. Comparative results of average consensus errors of angular rotations $\theta_{mi} - \sum_{i=1}^6 \theta_{mi}$, $i = 1, \dots, 6$ of each motor in Case I.

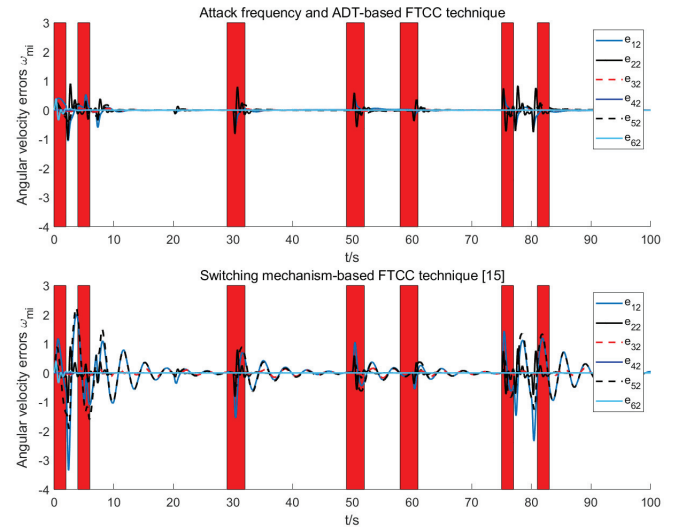


Fig. 5. Comparative results of average consensus errors of angular velocities $\omega_{mi} - \sum_{i=1}^6 \omega_{mi}$, $i = 1, \dots, 6$ of each motor in Case I.

Fig. 12 and Fig. 13. The triggering instants of the events under short-term DoS interval in Case I and long-term DoS interval in Case II are illustrated in Fig. 14 and Fig. 15. Compared with using resilient observers to estimate actuator faults [24], the ALO-CLE scheme proposed in the FTCC framework is more accurate in fault estimation. For short-term DoS interval, there is no deviation oscillations at the fault occurrence time 80s in Fig. 16, and for long-term DoS interval, there is no deviation oscillation at the fault occurrence time 40s and 60s in Fig. 17. These illustrations demonstrate that the errors in angular velocity and position consensus are capable of asymptotic convergence in addition to the sharp oscillation imbalance at some fault occurrence or DoS activation moments via the distributed event-triggered FTCC algorithm regardless of the complicated actuator faults in manipulators 1, 2, 3 and 5.

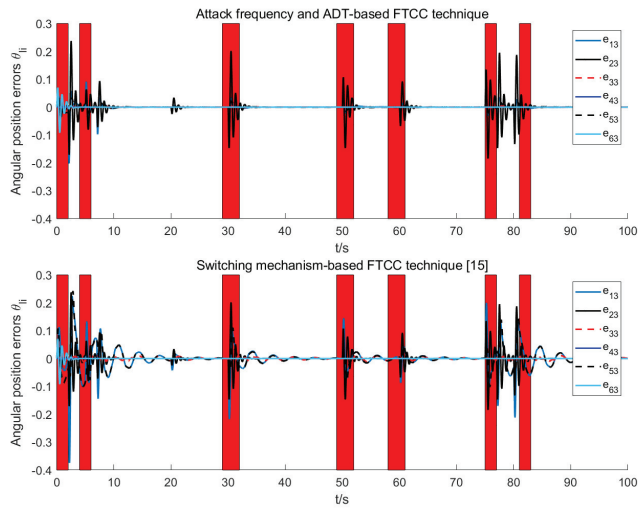


Fig. 6. Comparative results of average consensus errors of angular positions $\theta_{li} - \sum_{i=1}^6 \theta_{li}, i = 1, \dots, 6$ of each link in Case I.

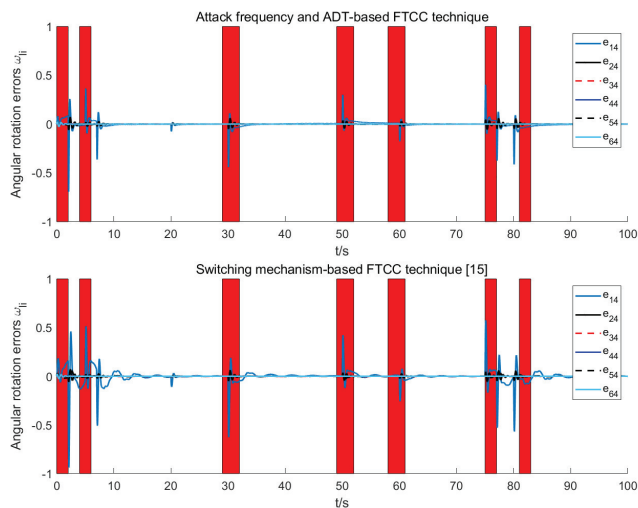


Fig. 7. Comparative results of average consensus errors of angular rotations $\omega_{li} - \sum_{i=1}^6 \omega_{li}, i = 1, \dots, 6$ of each link in Case I.

V. CONCLUSION

To ensure exponential consensus of MASSs, this study proposes an integrated co-design framework that integrates ALO-CLE-based decentralized FE and RBS-OLE-based distributed FTCC, focusing on countering aperiodic DoS attacks in networked hierarchy and complex incipient and abrupt actuator faults in physical hierarchy. The distributed FTCC law based upon state and fault estimations from FE protocol and adjacency broadcasting information at each past event-triggered instant is proposed in FTCC activation/DoS attack sleeping and FTCC sleeping/DoS attack activation cases. The sufficient criteria of attack frequency and ADT technique is proposed to achieve the prescribed anti-attack consensus performance and multistep calculation is illustrated to derive gain parameters in the distributed event-triggered FTCC solution. Future studies of more general nonlinear leader-following MASSs towards more effective anti-attack and tolerance capabilities in the face of sensor faults, DoS attacks, and even deception attacks are

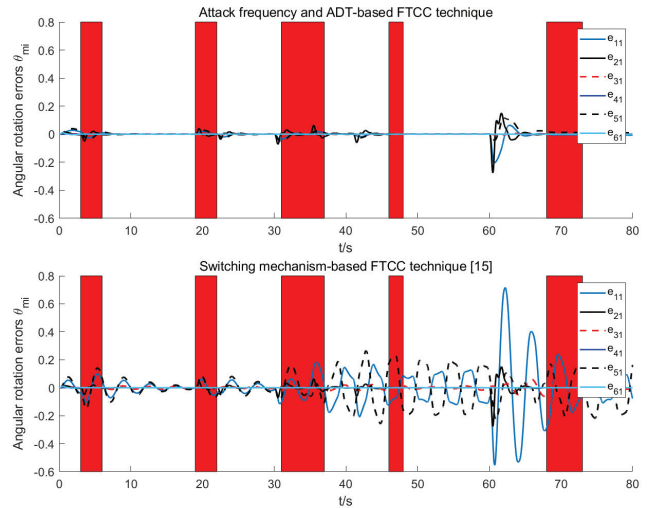


Fig. 8. Comparative results of average consensus errors of angular rotations $\theta_{mi} - \sum_{i=1}^6 \theta_{mi}, i = 1, \dots, 6$ of each motor in Case II.

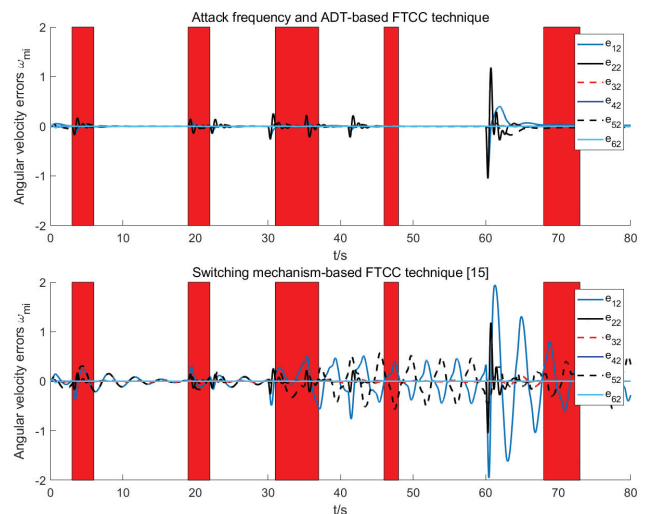


Fig. 9. Comparative results of average consensus errors of angular velocities $\omega_{mi} - \sum_{i=1}^6 \omega_{mi}, i = 1, \dots, 6$ of each motor in Case II.

highlighted. More challenges of fault-tolerant tracking issues with a substantial reduction in computational resources should be further addressed by the improved integration of cooperative FE and FTCC schemes with event-triggered mechanisms when message transmission fails intermittently.

REFERENCES

- [1] J. H. Qin, Q. C. Ma, Y. Shi, and L. Wang, "Recent advances in consensus of multi-agent systems: a brief survey," *IEEE Trans. Ind. Electron.*, vol. 64, no. 6, pp. 4972-4983, 2017.
- [2] W. H. Li, L. Shi, M. J. Shi, B. X. Lin, and K. Y. Qin, "Seeking velocity-free consensus for multi-agent systems with nonuniform communication and measurement delays," *IEEE Trans. Signal Inf. Proc. Netw.*, vol. 9, pp. 295-303, 2023.
- [3] Q. L. Wang, H. E. Psillakis, and C. Y. Sun, "Adaptive cooperative control with guaranteed convergence in time-varying networks of nonlinear dynamical systems," *IEEE Trans. Cybern.*, vol. 50, no. 12, pp. 5035-5046, 2020.
- [4] E. Bernuau, E. Moulay, P. Coirault, and F. Isfoula, "Practical consensus of homogeneous sampled-data multiagent systems," *IEEE Trans. Autom. Control*, vol. 64, no. 11, pp. 4691-4697, 2019.

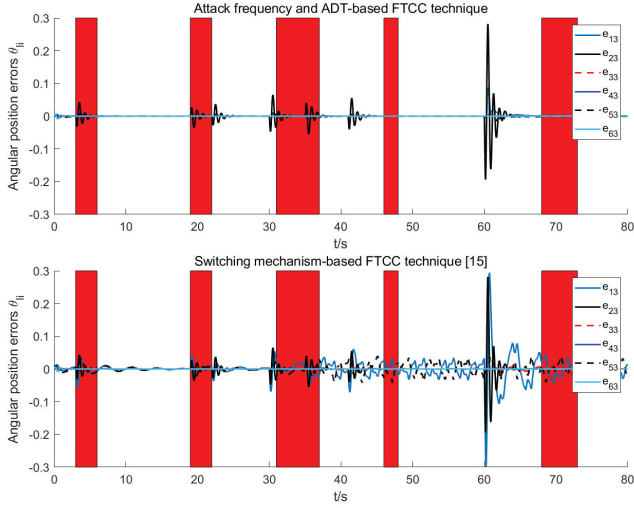


Fig. 10. Comparative results of average consensus errors of angular positions $\theta_{li} - \sum_{i=1}^6 \theta_{li}$, $i = 1, \dots, 6$ of each link in Case II.

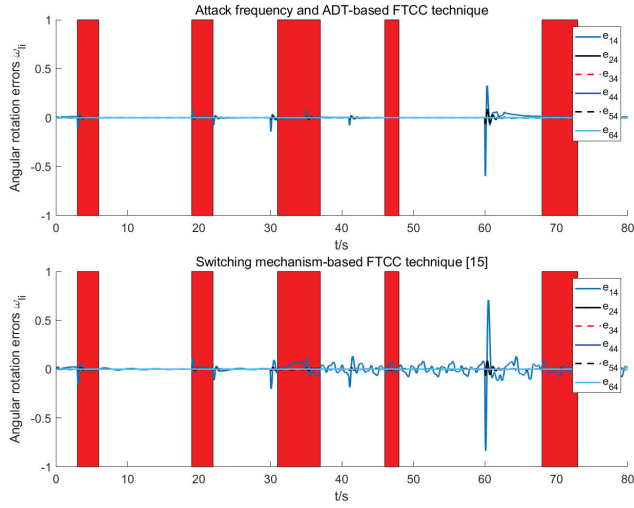


Fig. 11. Comparative results of average consensus errors of angular rotations $\theta_{li} - \sum_{i=1}^6 \theta_{li}$, $i = 1, \dots, 6$ of each link in Case II.

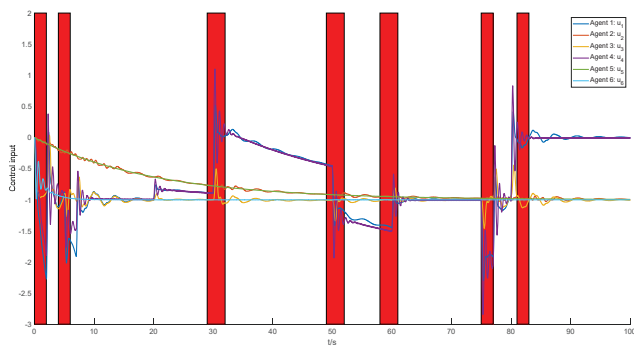


Fig. 12. Controller response curve under short-term DoS interval in Case I.

- [5] L. D. Alvergue, A. Pandey, G. X. Gu, and X. Chen, "Consensus control for heterogeneous multiagent systems," *SIAM J. Control Optim.*, vol. 54, no. 3, pp. 1719-1738, 2016.
- [6] W. B. Zhang, Z. D. Wang, Y. R. Liu, D. R. Ding, and F. E. Alsaadi, "Sampled-data consensus of nonlinear multiagent systems subject to

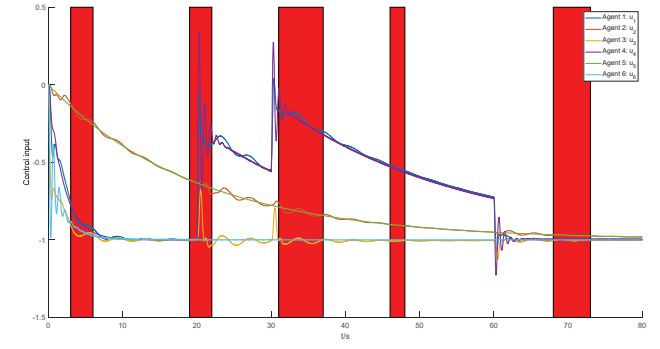


Fig. 13. Controller response curve under long-term DoS interval in Case II.

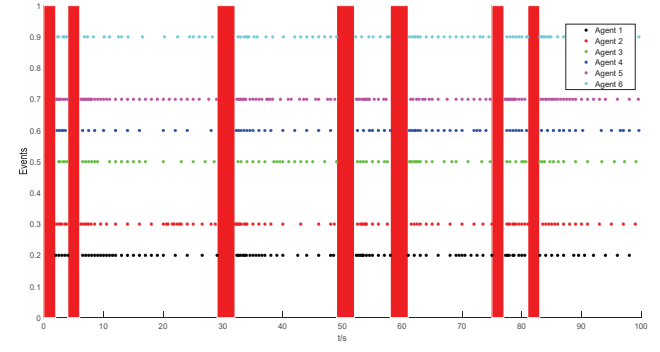


Fig. 14. Occurrences of the events under short-term DoS interval in Case I.

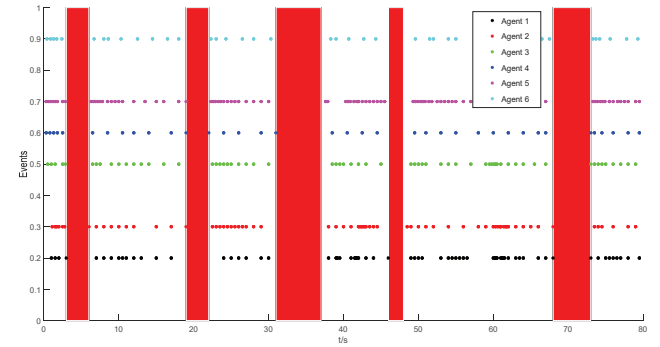


Fig. 15. Occurrences of the events under long-term DoS interval in Case II.

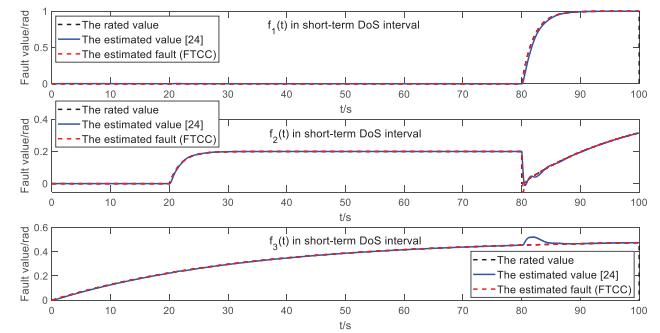


Fig. 16. Fault estimation comparison of [24] and ALO-CLE in Case I.

- cyber attacks," *Int. J. Robust Nonlinear Control*, vol. 28, no. 1, pp. 53-67, 2018.
- [7] X. G. Guo, D. Y. Zhang, J. L. Wang, J. H. Park, and L. Guo, "Observer-based event-triggered composite anti-disturbance control for multi-agent

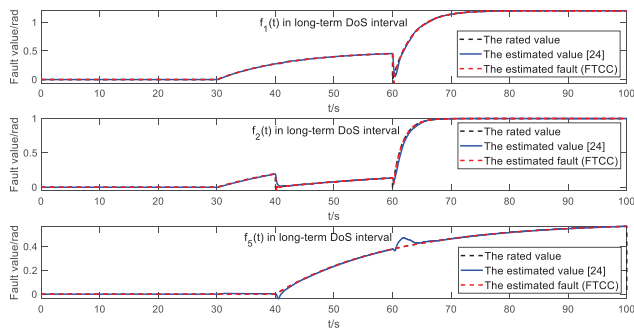


Fig. 17. Fault estimation comparison of [24] and ALO-CLE in Case II.

- systems under multiple disturbances and stochastic FDIAs,” *IEEE Trans. Autom. Sci. Eng.*, vol. 20, no. 1, pp. 528-540, 2023.
- [8] Y. Yang, X. Wang, and Y. F. Li, S. Gorbachev, and D. Yue, “Adaptive resilient tracking control with dual-terminal dynamic-triggering for a linear multi-agent system against false data injection attacks,” *IEEE Trans. Signal Inf. Proc. Netw.*, 2023. DOI: 10.1109/TSPN.2023.3239686.
- [9] C. Z. Hu, S. B. Ding, and X. P. Xie, “Event-based distributed set-membership estimation for complex networks under deception attacks,” *IEEE Trans. Autom. Sci. Eng.*, 2023. DOI: 10.1109/TASE.2023.3284448.
- [10] D. Zhang, L. Liu, and G. Feng, “Consensus of heterogeneous linear multiagent systems subject to aperiodic sampled-data and DoS attack,” *IEEE Trans. Cybern.*, vol. 49, no. 4, pp. 1501-1511, 2019.
- [11] X. G. Guo, D. Y. Zhang, J. L. Wang, and C. K. Ahn, “Adaptive memory event-triggered observer-based control for nonlinear multi-agent systems under DoS attacks,” *IEEE-CAA J. Automatica Sin.*, vol. 8, no. 10, pp. 1644-1656, 2021.
- [12] Y. Xu, M. Fang, P. Shi, and Z. G. Wu, “Event-based secure consensus of multiagent systems against DoS attacks,” *IEEE Trans. Cybern.*, vol. 50, no. 8, pp. 3468-3476, 2020.
- [13] M. Y. Huang, K. F. E. Tsang, Y. Z. Li, L. Li, and L. Shi, “Strategic DoS attack in continuous space for cyber-physical systems over wireless networks,” *IEEE Trans. Signal Inf. Proc. Netw.*, vol. 8, pp. 421-432, 2022.
- [14] S. Y. Ren, R. Mao, and J. G. Wu, “Passivity-based leader-following consensus control for nonlinear multi-agent systems with fixed and switching topologies,” *IEEE Trans. Netw. Sci. Eng.*, vol. 6, no. 4, pp. 844-856, 2019.
- [15] C. Liu, B. Jiang, K. Zhang, and R. J. Patton, “Distributed fault-tolerant consensus tracking control of multi-agent systems under fixed and switching topologies,” *IEEE Trans. Circuits Syst. I-Regul. Pap.*, vol. 68, no. 4, pp. 1646-1658, 2021.
- [16] Z. H. Wu, S. Jiang, and L. B. Xie, “Fault-tolerant finite-time consensus of multi-agent systems under asynchronous self-sensing function failures,” *IEEE Trans. Signal Inf. Proc. Netw.*, vol. 9, pp. 477-489, 2023.
- [17] Y. Liu and G. H. Yang, “Fixed-time fault-tolerant consensus control for multi-agent systems with mismatched disturbances,” *Neurocomputing*, vol. 366, pp. 154-160, 2019.
- [18] Y. J. Wang, Y. D. Song, and F. L. Lewis, “Robust adaptive fault-tolerant control of multiagent systems with uncertain nonidentical dynamics and undetectable actuation failures,” *IEEE Trans. Ind. Electron.*, vol. 62, no. 6, pp. 3978-3988, 2015.
- [19] M. Khalili, X. D. Zhang, Y. C. Cao, M. M. Polycarpou, and T. Parisini, “Distributed fault-tolerant control of multiagent systems: an adaptive learning approach,” *IEEE Trans. Neural Netw. Learn. Syst.*, vol. 31, no. 2, pp. 420-432, 2020.
- [20] F. B. Cheng, H. J. Liang, H. Q. Wang, G. D. Zong, and N. Xu, “Adaptive neural self-triggered bipartite fault-tolerant control for nonlinear MASs with dead-zone constraints,” *IEEE Trans. Autom. Sci. Eng.*, vol. 20, no. 3, pp. 1663-1674, 2023.
- [21] G. G. Wen, X. Q. Zhai, Z. X. Peng, and A. Rahmani, “Fault-tolerant secure consensus tracking of delayed nonlinear multi-agent systems with deception attacks and uncertain parameters via impulsive control,” *Commun. Nonlinear Sci. Numer. Simul.*, vol. 82, 105043, 2020.
- [22] L. Zhao and G. H. Yang, “Cooperative adaptive fault-tolerant control for multi-agent systems with deception attacks,” *J. Frankl. Inst.*, vol. 357, no. 6, pp. 3419-3433, 2020.
- [23] Y. Li, H. Fang, and J. Chen, “Anomaly detection and identification for multiagent systems subjected to physical faults and cyberattacks,” *IEEE Trans. Ind. Electron.*, vol. 67, no. 11, pp. 9724-9733, 2020.
- [24] C. Deng and C. Y. Wen, “Distributed resilient observer-based fault-tolerant control for heterogeneous multiagent systems under actuator faults and DoS attacks,” *IEEE Trans. Control Netw. Syst.*, vol. 7, no. 3, pp. 1308-1318, 2020.
- [25] S. K. Liu, B. Jiang, Z. H. Mao, and Y. M. Zhang, “Neural-network-based adaptive fault-tolerant cooperative control of heterogeneous multiagent systems with multiple faults and DoS attacks,” *IEEE Trans. Neural Netw. Learn. Syst.*, 2023. DOI: 10.1109/TNNLS.2023.3282234.
- [26] L. Zhao and G. H. Yang, “Adaptive fault-tolerant control for nonlinear multi-agent systems with DoS attacks,” *Inf. Sci.*, vol. 526, pp. 39-53, 2020.
- [27] Z. X. Zhang and J. X. Dong, “Fault-tolerant containment control for IT2 fuzzy networked multiagent systems against denial-of-service attacks and actuator faults,” *IEEE Trans. Syst. Man Cybern. -Syst.*, vol. 52, no. 4, pp. 2213-2224, 2022.
- [28] T. Dong and Y. L. Gong, “Leader-following secure consensus for second-order multi-agent systems with nonlinear dynamics and event-triggered control strategy under DoS attack,” *Neurocomputing*, vol. 416, pp. 95-102, 2020.
- [29] J. K. Ni, F. Y. Duan, and P. Shi, “Fixed-time consensus tracking of multiagent system under DOS attack with event-triggered mechanism,” *IEEE Trans. Circuits Syst. I-Regul. Pap.*, vol. 69, no. 12, 5286-5299, 2022.
- [30] C. Peng, J. Zhang, and Q. L. Han, “Consensus of multiagent systems with nonlinear dynamics using an integrated sampled-data-based event-triggered communication scheme,” *IEEE Trans. Syst. Man Cybern. -Syst.*, vol. 49, no. 3, pp. 589-599, 2019.
- [31] Y. Fan, L. Liu, G. Feng, and Y. Wang, “Self-triggered consensus for multi-agent systems with zeno-free triggers,” *IEEE Trans. Autom. Control*, vol. 60, no. 10, pp. 2779-2784, 2015.
- [32] S. L. Li, Y. Z. Chen, and P. X. Liu, “Fault estimation and fault-tolerant tracking control for multi-agent systems with lipschitz nonlinearities using double periodic event-triggered mechanism,” *IEEE Trans. Signal Inf. Proc. Netw.*, vol. 9, pp. 229-241, 2023.
- [33] Z. H. Cheng, D. Yue, S. L. Hu, H. Ge, and L. Chen, “Distributed event-triggered consensus of multi-agent systems under periodic DoS jamming attacks,” *Neurocomputing*, vol. 400, pp. 458-466, 2020.
- [34] Y. Xu, M. Fang, Z. G. Wu, Y. J. Pan, M. Chadli, and T. W. Huang, “Input-based event-triggering consensus of multiagent systems under denial-of-service attacks,” *IEEE Trans. Syst. Man Cybern. -Syst.*, vol. 50, no. 4, pp. 1455-1464, 2020.
- [35] D. X. Chen, X. L. Liu, W. W. Yu, L. Zhu, and Q. P. Tang, “Neural-network based adaptive self-triggered consensus of nonlinear multi-agent systems with sensor saturation,” *IEEE Trans. Netw. Sci. Eng.*, vol. 8, no. 2, pp. 1531-1541, 2021.